JOURNAL OF GEOPHYSICAL RESEARCH, VOL. 106, NO. D5, PAGES 4797-4814, MARCH 16, 2001

From molecular clusters to nanoparticles: Role of ambient ionization in tropospheric aerosol formation

Fangqun Yu[1] and Richard P. Turco

Department of Atmospheric Sciences, University of California, Los Angeles, California

Abstract. We investigate the role of background ionization, associated mainly with galactic cosmic radiation, in the generation and evolution of ultrafine particles in the marine boundary layer. We follow the entire course of aerosol evolution, from the initial buildup of molecular clusters (charged and uncharged) through their growth into stable nanoparticles. The model used for this purpose is based on a unified collisional (kinetic) mechanism that treats the interactions between vapors, neutral and charged clusters, and particles at all sizes. We show that air ions are likely to play a central role in the formation of new ultrafine particles. The nucleation of aerosols under atmospheric conditions involves a series of competing processes, including molecular aggregation, evaporation, and scavenging by preexisting particles. In this highly sensitive nonlinear system, electrically charged embryos have a competitive advantage over similar neutral embryos. The charged clusters experience enhanced growth and stability as a consequence of electrostatic interactions. Simulations of a major nucleation event observed during the Pacific Exploratory Mission (PEM) Tropics-A can explain most of the observed features in the ultrafine particle behavior. The key parameters controlling this behavior are the concentrations of precursor vapors and the surface area of preexisting particles, as well as the background ionization rate. We find that systematic variations in ionization levels due to the modulation of galactic cosmic radiation by the solar cycle are sufficient to cause a notable variation in aerosol production. This effect is greatest when the ambient nucleation rate is limited principally by the availability of ions. Hence we conclude that the greatest influence of such ionization is likely to occur in and above the marine boundary layer. While a systematic change in the ultrafine particle production rate is likely to affect the population of cloud condensation nuclei and hence cloud optical properties, the magnitude of the effect cannot be directly inferred from the present analysis, and requires additional analysis based on specific aerosol-cloud interactions.

1. Introduction

Tropospheric aerosols affect the Earth's radiation budget directly by reflecting and absorbing shortwave solar radiation [*Charlson et al.*, 1992] and indirectly by serving as cloud condensation nuclei, thereby influencing the optical properties and lifetimes of clouds [*Twomey*, 1977]. At the present time, the uncertainty in aerosol radiative forcing is large enough to compensate for most of the effect of greenhouse gases [*Intergovernmental Panel on Climate Change (IPCC)*, 1996]. The magnitude of aerosol radiative forcing is sensitive to particle size and concentration, which are influenced by nucleation processes. However, the origin of ultrafine aerosols throughout the troposphere has not yet been determined despite intense research over several decades. Moreover, even the fundamental mechanisms that lead to new particle formation remain poorly understood.

The classical theory of binary sulfuric acid and water nucleation, which has been widely applied in the past, cannot explain many of the observations of particle formation in the lower atmosphere [e.g., *Covert et al.*, 1992; *Hoppel et al.*, 1994; *Weber et al.*, 1996, 1997, 1998; *Clarke et al.*, 1998]. Typically, the nucleation rates predicted by classical binary homogeneous nucleation (BHN) theory are much lower (by a factor of up to ~10^{10}) than the rates inferred from simultaneous measurements of freshly nucleated nanoparticles and sulfuric acid gas concentrations [e.g., *Weber et al.*, 1996; *Clarke et al.*, 1998].

Ternary homogeneous nucleation (THN), involving ammonia as well as sulfuric acid [*Coffman and Hegg*, 1995; *Korhonen et al.*, 1999], has been suggested as a means of accelerating the nucleation process [e.g., *Weber et al.*, 1998; *Clarke et al.*, 1998; *Kulmala et al.*, 2000]. In this case, ammonia stabilizes the critical embryo (reducing its size) and thus significantly increases the nucleation rate calculated from classical theory. *Kulmala et al.* [2000], for example, have estimated ternary nucleation rates averaging ~ 100 $cm^{-3}s^{-1}$, and as large as $3.5x10^4 cm^{-3}s^{-1}$ (which are larger than H_2SO_4 production rates under ambient tropospheric conditions). They propose that THN generates thermodynamically stable clusters (TSCs) of 1 nm diameter, which will be present at concentrations as high as ~10^5 cm^{-3} throughout the lower troposphere. TSCs can have concentrations reaching 10^7 cm^{-3} on certain occasions. The THN theory, however, does not consider the initial buildup of the molecular clusters from the vapor phase and instead assumes that 1-nm TSCs appear at the calculated nucleation rate. In reality, the growing subcritical neutral sulfuric acid/ammonia embryos must compete for vapor with other more

[1] Now at Atmospheric Sciences Research Center, State University of New York, Albany, New York.

Paper number 2000JD900539.
0148-0227/01/2000JD900539$09.00

thermodynamically stable species, such as ions and charged clusters (see section 2).

There is a further problem with both the BHN and THN mechanisms. The subsequent growth rate of newly formed nanoparticles, which is assumed to be driven by the condensation of H_2SO_4 together with H_2O and NH_3, appears to be a factor of ~10 too low to explain the appearance of new ultrafine aerosols by midday, or before [e.g., *Weber et al.*, 1997, 1998; *Turco and Yu*, 2000]. *Kulmala et al.* [2000] show that the formation of stable neutral embryos by THN will not generally lead to many 3-nm particles unless at least one other condensable species is available at a sufficiently high concentration. These circumstances, however, also increase the likelihood that ion nucleation and growth will occur (section 2).

In the past, researchers in various fields have alluded to ions as potential nucleation embryos [e.g., *Mohnen*, 1971; *Arnold*, 1980; *Hamill et al.*, 1982]. It has also been noted that ion activation should precede homogeneous nucleation under atmospheric conditions, since condensation onto ions is generally favored [e.g., *Raes et al.*, 1986; *Hoppel et al.*, 1994]. However, quantitative studies of the role of ions in tropospheric particle formation, using models validated against observations specific to background conditions, have been lacking.

Recent work by *Yu and Turco* [2000a] demonstrates that charged molecular clusters, condensing around natural air ions, can grow significantly faster than corresponding neutral clusters and thus can preferentially achieve stable, observable sizes. A clear example of the strong influence electrification exercises on charged clusters and nanoparticles is noted in aircraft wakes, where combustion chemiions rapidly evolve into a distinct "ion-mode" of "volatile" particles [*Yu and Turco*, 1997]. The chemiion theory predicts the complex behavior of aircraft aerosols [*Yu et al.*, 1998, 1999; *Kärcher et al.*, 1998], and is supported by measurements of massive ion clusters in fresh plumes [e.g., *Arnold et al.*, 1998a, 1998b, 1999, 2000; *Wohlfrom et al.*, 2000]. In the case of particle formation on ambient ions, the processes are similar in most respects to those controlling aircraft aerosols, although occurring at different time scales, species concentrations, and temperatures. In fact, the physics that underlies the ion-mediated nucleation (IMN) model developed by *Yu and Turco* [2000a] for tropospheric conditions is derived directly from the microphysics used to simulate aircraft emissions. In both applications a fundamental kinetic approach is applied to calculate cluster formation and growth rates. Significantly, the resulting general mechanism seems to account consistently for ultrafine aerosol formation in jet plumes and in clean continental air [*Weber et al.*, 1997], as well as for the observed diurnal variation in the atmospheric mobility spectrum [*Hõrrak et al.*, 1998], as demonstrated by *Yu and Turco* [2000a].

In this paper, we discuss the fundamental physical concepts that are employed in the IMN theory and analyze recent data on boundary layer aerosol formation. It is argued that a kinetic approach is required to study particle nucleation in ambient environments, because the interactions between vapors, neutral clusters, and charged species are all potentially important under variable conditions. The IMN theory, and its basic kinetic formulation, are applied here to study a particle nucleation "burst" observed in the tropical marine boundary layer during NASA's Pacific Exploratory Mission (PEM) Tropics-A [*Clarke et al.*, 1998]. The comprehensive PEM measurements provide real-time information that constrains a variety of key parameters, including dimethylsulfide, sulfur dioxide, sulfuric acid (vapor), hydroxyl radical and ozone concentrations, temperature, relative humidity, aerosol size distribution, and total aerosol surface area. For the conditions prevailing at the time of the experiment, classical binary homogeneous nucleation rates would have been negligible [*Clarke et al.*, 1998]. Ammonia concentrations were not available to constrain directly a ternary nucleation mechanism.

2. Ions, Cluster Growth, and Aerosol Formation

The proposed concept for aerosol formation and evolution in the lower atmosphere, including the effects of ions, is illustrated schematically in Figure 1. Ambient ions are continuously generated by galactic cosmic rays (GCRs) at the rate of ~2 ion-pairs $cm^{-3}s^{-1}$ at ground level and up to ~20-30 ion-pairs $cm^{-3}s^{-1}$ in the upper troposphere [*Reiter*, 1992]. Note that the GCR component of the ionization rate is a function of altitude and latitude and is distinctly modulated by solar activity (see below). Ions can also be generated by other localized sources (such as radioactive emanations, lightning, corona discharge, combustion, etc.). The actual ionization rate near the surface over land, for example, can be five times or more greater than that due to cosmic rays alone, owing to natural radioactivity from soils. In the present study of boundary layer aerosol formation over the oceans, GCRs are the dominant source of ionization.

The initial primary ions quickly react with common air constituents to generate a series of increasingly stable "terminal" ions, such as HSO_4^-. When certain vapors such as H_2SO_4, H_2O, NH_3, and numerous organic species are available, the core terminal ions rapidly accumulate ligands to form a continuous distribution of charged clusters. If a ligand vapor is sufficiently supersaturated with respect to its condensed phase, a significant fraction of the ion clusters can be nucleated and grow into ultrafine particles.

Ion-ion recombination limits the concentration of "small" ions, which consist of the simple terminal molecular core ions and their stable clustered forms. Any charged (neutral) particles that are present are eventually neutralized (charged) by attracting small ions or other charged particles. Each recombination event results in a neutral cluster, some of which may be thermodynamically stable and continue to grow to measurable sizes [*Turco et al.*, 1998].

In parallel with ion clustering, growth, and recombination a number of ambient vapors will also aggregate kinetically to form a distribution of neutral clusters. Indeed, if conditions are favorable, some of the these clusters will reach critical size and "nucleate" homogeneously, while the others will tend to evaporate. Since there is very little information available to define the thermodynamic properties of small neutral molecular clusters consisting of water, acids, and bases like ammonia, it is not yet possible to predict their stability or likely composition with confidence, even for clusters composed of only two or three molecules, let alone tens of molecules.

The situation is quite different in the case of ion clusters, however, where extensive laboratory-based, as well as field-derived, thermodynamic data are available for a wide range of ligands. This is a consequence of the inherent stability of these charged species. Since classical nucleation theory depends on a knowledge of the thermodynamics of relatively small molecular clusters (which are electrically neutral in the case of homogeneous nucleation, and charged in the case of ion nucleation), classical predictions can be notoriously unreliable, especially in the homogeneous case [e.g., *Hamill et al.*, 1982]. Classical theory also assumes a pseudo steady state distribution of clusters (and hence a fixed concentration of critical embryos), which is achieved "instantane-

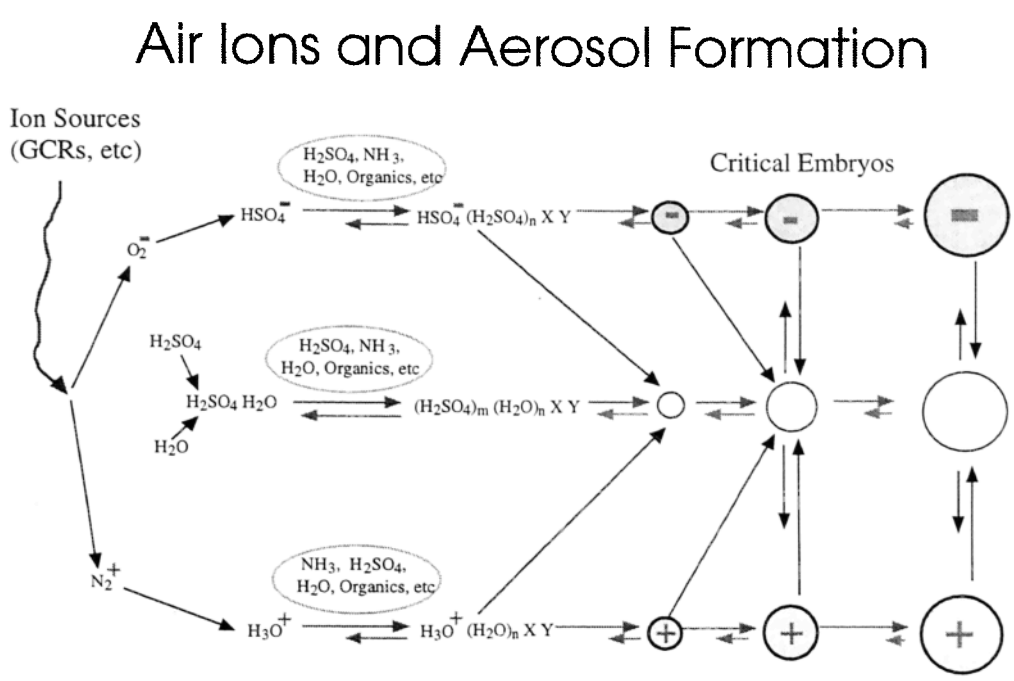

Figure 1. Schematic diagram showing the possible role of air ions in particle formation. Enhanced stability and growth rates (consequences of electrostatic forces) provide a key competitive advantage to electrically charged embryos over neutral clusters. Under the proper conditions, charged nanoparticles will preferentially achieve observable sizes. The recombination of charged species offers another possible pathway to stable embryo formation in the troposphere [*Turco et al.*, 1998].

ously," even as the precursor vapor concentrations change. Accordingly, there are circumstances for which classical nucleation theory may greatly overestimate (or underestimate) the rates of particle formation.

The buildup of molecular clusters is always kinetically limited; in fact, this is one of the most fundamental limitations to particle formation. Under ambient conditions the production of binary H_2SO_4-H_2O aggregates (or H_2SO_4-H_2O-NH_3 clusters in the ternary system) is controlled by molecular collision rates, accommodation coefficients, and thermal stability, each of which can inhibit cluster growth. The kernels for neutral molecular collisions are ~10^{-10} cm^3s^{-1}, assuming perfect sticking of the impinging molecules. More typically, accommodation coefficients <1 are expected for small clusters. On the other hand, if a cluster is charged, the collision kernel can be significantly enhanced by electrostatic effects. It is well known, for example, that ion-molecule reaction rate coefficients are ~10^{-9} cm^3s^{-1} (implying very efficient accommodation).

The ambient concentration of small atmospheric ions (positive or negative) in the lower atmosphere is ~1000 cm^{-3} [e.g., *Viggiano*, 1993]. In situations where "slow" nucleation events are encountered, typical H_2SO_4 vapor concentrations are $\leq 10^7$ cm^{-3} [*Weber et al.*, 1996, 1997, 1998, 1999; *Clarke et al.*, 1999]. The relative importance of various kinetic processes involving the species of interest can be estimated by considering an upper-limit neutral-neutral molecular collision coefficient of 2x 10^{-10} cm^3s^{-1}, ion-neutral reaction coefficient of 2x10^{-9} cm^3s^{-1}, and ion-ion recombination coefficient of 2x10^{-6} cm^3s^{-1}. For the species abundances stated, the time required for a small ion to be neutralized is ~1000 s, and the time needed for an ion to attract an H_2SO_4 molecule is ~50 s. Hence, prior to neutralization, an ion could accumulate sufficient H_2SO_4 (up to 20 molecules) to create a typical critical embryo, and thus be nucleated. Here it is presumed that the collision kernel is only a weak function of cluster size, and a unit accommodation coefficient applies to exothermic ion-neutral encounters [*Yu and Turco*, 1998]. Such rapid aggregation could occur even in the absence of ammonia, or other stabilizing species. In reality, ammonia, organic vapors, and similar materials commonly found in the atmosphere will be strongly attracted to ion clusters, leading to greater stability and kinetically limited growth (that is, growth without dissociation; see below).

By contrast, a neutral H_2SO_4 molecule would form an H_2SO_4 dimer after ~500 s, for a unit accommodation coefficient. However, the effective sticking coefficient for molecular collisions is usually much smaller than unity, which also likely holds for collisions of molecules with clusters lying below the size of the critical embryo [*Yu and Turco*, 1998]. For example, *Ianni and Bandy* [2000] recently carried out ab initio calculations for small sulfuric acid/water clusters, concluding that the formation of neutral H_2SO_4 dimers from monomers is strongly inhibited kinetically and thermodynamically due to the rapid dissociation of H_2SO_4 collision complexes under typical conditions in the lower atmosphere. These physical limitations further extend the time required for neutral clusters to grow. It follows that for the conditions stated, the time needed to assemble a neutral critical embryo would be much longer than that required to form a charged embryo. This discussion ignores the scavenging of clusters by ambient particles, and the evaporation of aggregates larger than a few

molecules. The scavenging rates for small charged or neutral clusters and particles depend on the surface area of the background aerosol. A large ambient surface area can suppress nucleation, as precursor vapors and small clusters are removed before they can achieve stable, observable sizes. In general, the smaller the cluster, the greater its tendency to be lost by either evaporation or scavenging.

The electrostatic enhancement in the rate of condensation of vapor onto charged clusters may be a critical factor in the generation of new condensation nuclei. The formation of sensible aerosols, in fact, is an outcome of the competition between the growth of new, stable particles and their scavenging by ambient aerosols. The neutralization of growing charged particles, while a mechanism that can add significant mass in the early stages of cluster evolution, may impede growth for clusters approaching the critical size. For typical ambient conditions, there is sufficient H_2SO_4 vapor available, however, to allow some of the larger ion clusters to evolve into rapidly growing nanoparticles. Neutral microclusters, on the other hand, will not in general surpass critical size because of their lower stability and slower growth rates.

It should be noted that the presence of ammonia vapor, as well as common tropospheric compounds such as acetone [*Arnold et al.*, 1997], methanol [*Fehsenfeld et al.*, 1978] and other organics [*Huertas et al.*, 1974] can further enhance the growth and nucleation of microscopic ion-aerosols. Ammonia efficiently reacts with and accumulates on ions [*Castleman et al.*, 1978; *Viggiano et al.*, 1980, 1988]. Hence ammonia vapor acts to stabilize growing ionic clusters (an effect also proposed for neutral clusters [*Korhonen et al.*, 1999]) for either sign of electrification. The resulting charged nanoparticles would themselves attract neutral clusters (including ammoniated embryos) that are produced in the same air mass. Further, it is apparent that the recombination of large ammoniated ions with acid-containing clusters could generate highly stable neutral products that may themselves participate in the nucleation process.

3. Kinetic Modeling of Subnanometer Particle Dynamics

3.1. Classical Theory Versus Molecular Kinetics

Two distinct approaches have been taken in simulating the formation of aerosols in the atmosphere. The standard "classical" formulation is based on the determination of the Gibbs free energy of a critical "embryo," or nucleus, using a "droplet" representation for molecular clusters up to and including the critical size [e.g., *Pruppacher and Klett*, 1978]. This so-called "capillarity" approximation assumes that a molecular cluster of any size can be reasonably characterized using the corresponding bulk properties of the condensed phase (in particular, the surface tension, density, and vapor pressure). Certainly, this approximation improves as the cluster grows to macroscopic dimensions (>>1 nm). The thermodynamic properties of classical embryos are determined by calculating the energy needed to assemble a liquid droplet (or solid sphere) having a specific radius or corresponding specific number of molecules. The dependence of the free energy on cluster radius allows an equilibrium Boltzmann distribution of cluster concentrations to be computed. Typically, a maximum in the free energy with increasing radius indicates that the critical nucleus has been reached. If one additional molecule is added to this nucleus, the resulting particle will, under the prevailing conditions, grow freely.

In the classical theory the number of critical nuclei is determined by adopting the equilibrium distribution, while the nucleation rate is calculated by assuming the collision of a monomer with the critical nucleus (with possible corrections for the presence of molecular dimers, trimers, etc., and for the depletion of critical nuclei owing to activation). Importantly, the critical nucleus appears instantaneously in this formulation (that is, the growth kinetics of the subcritical embryos is neglected and hence is implicitly assumed to be rapid relative to other relevant time scales). In practice, the activated nuclei are inserted into the first bin of a sectional aerosol model, or into the "nucleation mode" of a moment-based model, to simulate the subsequent growth by condensation and coagulation. These latter approximations may themselves introduce further errors, including "numerical diffusion."

The second technique for treating aerosol formation, which is outlined here, is the kinetic approach. In this case, the entire history of cluster growth is treated as a sequence of fundamental collisional steps beginning with the vapor phase (although in the presence of pre-existing aerosols, if necessary). Then, coagulation and dissociation, extrapolated to molecular scales, represent the key processes driving aerosol evolution. In this sense, condensation and coagulation are analogous, where condensation (evaporation) is equivalent to the coagulation (dissociation) of a molecule or small molecular cluster with (from) a particle.

The classical approach is popular because it provides a simple, cognitive model, from which analytical and numerical solutions are readily derived. However, problems with this method include the assumed instantaneous appearance of critical nuclei, reliance on bulk properties that clearly do not apply to small prenucleation clusters, lack of thermodynamic data for mixtures, and predicted rates of nucleation that are effectively unconstrained and extraordinarily sensitive to small adjustments in thermodynamic parameters (in fact, the uncertainty in typical classical H_2SO_4-H_2O binary nucleation rates may extend over 10 orders of magnitude or more [*Hamill et al.*, 1982]). Further, the common necessity for "tuning" factors, ranging in value from 10^{-5} to 10^{7} [e.g., *Wyslouzil et al.*, 1991; *Raes et al.*, 1992; *Russell et al.*, 1994; *Kulmala et al.*, 1998; *Capaldo* et al., 1999], to calculate such binary nucleation rates suggests that the classical theory is inherently unreliable under atmospheric conditions. We recognize that in the environment, precursor vapors such as sulfuric acid are continuously varying, always at low concentrations. Hence assumptions of unconstrained growth and instantaneous equilibrium are unlikely to prove reasonable.

The kinetic approach is superior to the classical approach in that it is physically more realistic and flexible. For example, absurdly high nucleation rates are not predicted by a kinetic model, due to the collisional limitations on particle growth at all stages of evolution. Accordingly, kinetic-based calculations should be less sensitive to uncertain thermodynamic properties than classical solutions. The main drawback of the kinetic scheme is that additional data are needed. Specifically, in a comprehensive treatment the collision kernel and dissociation coefficient for each distinct cluster would be required. A number of simplifications can, nevertheless, lead to a tractable model. For example, as in the classical approach, bulk properties can be assigned to small clusters to estimate kinetic coefficients (again, the particle formation rates subsequently predicted by the kinetic model are not as sensitive to this assumption as are those predicted by the classical approach). The main source of uncertainty in the kinetic approach is related to the "sticking" efficiency during the interaction between small clusters and molecules (see below).

A significant advantage of the kinetic approach over classical nucleation theory is the ability to deal with both charged and neu-

tral species at all sizes in a straightforward and self-consistent manner. In the classical theory, nucleation of charged and neutral particles occurs instantaneously, simultaneously, and independently. In fact, the interacting system of vapor, ions, charged and neutral clusters, and preexisting aerosols can evolve along many possible routes and produce a broad range of outcomes. A kinetic model allows the role of ambient ionization on the rates of particle formation and growth to be addressed explicitly. This is a crucial point, since electrical forces appear to play an important (if not dominant) role in aerosol formation under a variety of conditions [e.g., *Yu and Turco*, 1997, 1998, 2000a, 2000b; *Yu et al.*, 1999; *Turco et al.*, 1998; *Turco and Yu*, 2000]. Electrical charge is especially important at very small cluster sizes, such as must occur during the initial stages of aerosol formation.

Measurements characterizing aerosol formation have become more sophisticated and specific in recent years. For example, simultaneous measurements of nanometer-size aerosols (as small as ~3 nm) and precursor sulfuric acid vapor concentrations [e.g., *Weber et al.*, 1996, 1997, 1998; *Clarke et al.*, 1998] now provide strong constraints on microphysical models. Moreover, new data on the properties of likely atmospheric pre-nucleation clusters [*Weber et al.*, 1995; *Eisele and Hanson*, 2000], and novel techniques for measuring air ions and charged molecular clusters in the sub-nanometer to several nanometer size range [*Aplin and Harrison*, 2000; *Gamero-Castaño and Fernández de la Mora*, 2000; *Lovejoy*, 1999; *Wohlfrom et al.*, 2000], are becoming available. Further, observations not previously considered, such as the mobility spectrum of air [*Hõrrak et al.*, 1998, 2000], offer a unique view of particle formation [*Yu and Turco*, 2000a]. To interpret this wider range of measurements, explicit kinetic modeling may be most appropriate.

3.2. An Advanced Particle Microphysics Model

To investigate the fundamental process leading to new particle production, the kinetic approach is applied in this study. A complete suite of interactions between neutral and charged clusters and particles, as well as their coupling to the vapor phase, has been integrated into an advanced particle microphysics (APM) code. This model tracks the compositions and size distributions of several different particle types (including both neutral and charged species). Previous publications describing applications of the APM model offer details about this approach [*Yu*, 1998; *Yu and Turco*, 1997, 1998, 2000a; *Kärcher et al.*, 1998; *Yu et al.*, 1998, 1999].

In the simulations that follow, the fine aerosols (charged and neutral) are taken to be composed of sulfuric acid and water in binary mixtures. The particle size distribution is represented using a hybrid bin structure, in which both "dry," and equivalent "wet," sizes are determined for each particle bin [*Jacobson and Turco*, 1995]. The dry size is that associated only with the sulfuric acid in the droplet (i.e., the size at 0% relative humidity). The first dry bin size is therefore set to the dimension of an H_2SO_4 molecule (~0.56 nm). The subsequent bins increase monotonically in size (volume), with the volumes of the second, third, fourth, and fifth bins being precisely 2, 3, 4, and 5 times that of the first bin. From bin 6 upward, the dry volume increases by a factor of 1.2 between adjacent bins, with the total range of dry particle sizes extending from 0.56 nm to 5 μm.

The equivalent wet size corresponding to each dry bin is calculated assuming instantaneous equilibrium of the sulfuric acid in the particle with the local ambient water vapor (at the prevailing temperature). This calculation is inherently uncertain for the smallest bins inasmuch as the thermodynamic properties of the small "start-up" clusters remain unquantified. Thus for example, the wet diameter of an average hydrated sulfuric acid molecule is roughly estimated to be 0.65 nm (in the present case; see section 4). The wet size of each dry bin is calculated by assuming the hygroscopic properties of sulfuric acid and water binary mixtures [e.g., *Hamill et al.*, 1982]. While this treatment ignores other potential components of the aerosol such as ammonia, it is not an important factor in the following simulations and discussion. The capability to extend this approach to more general aerosol mixtures is included in the APM [*Jacobson et al.*, 1996].

3.3. Collisional Parameters for Kinetic Modeling

In the kinetic approach, coagulation (extrapolated to molecular scales) is the key process driving nanoparticle evolution. Evaporation, or dissociation, of the smallest clusters is also obviously of importance. The coagulation kernel is the key parameter to be specified, in which two clusters or particles undergoing relative motion come into contact and fuse. However, there are a number of difficulties in determining the collision kernels across the entire range of sizes and charge states of interest. Three key factors must be specified for each cluster pair: the collision kernel, accommodation coefficient, and evaporation or dissociation coefficient. These parameters, although related, are often addressed separately in microphysical discussions. The most difficult process to characterize is cluster dissociation. Practically speaking, this is equivalent to vapor evaporation, since only monomers are likely to escape a cluster or particle surface under atmospheric conditions. The approximations used in the current version of the APM model are discussed below.

3.3.1. Collisional (coagulation) kernel. Coagulation kernels for particles at all sizes have been a subject of research for decades, owing to the importance of aerosols in a number of fields of science, engineering and medicine [*Fuchs*, 1964]. For sensible particles (>>1 nm in size), the relative motion is induced by thermal agitation (Brownian motion), gravitational sedimentation, and turbulence. The present coagulation model treats all of these processes using well-developed analytic approaches [e.g., *Fuchs*, 1964; *Turco et al.*, 1979]. Brownian coagulation is the dominant mechanism for ultrafine particles. We adopt Fuchs' basic formula [*Fuchs*, 1964] to calculate the Brownian coagulation kernel for neutral particle encounters.

For small charged clusters and nanoparticles the rate of coalescence is strongly influenced by electrostatic attraction and repulsion. There are two common methods employed to calculate the effects of charge on the coagulation kernels. We rely on a theory that explicitly treats image capture and three-body trapping effects [e.g., *Hoppel and Frick*, 1986], as opposed to the limiting-sphere approximation [*Fuchs*, 1964]. Even so, differences between the coagulation kernels calculated by these methods lie within the uncertainty bounds of available laboratory data on coagulation rates in the nanometer size range [*Reischl et al.*, 1986]. The original calculations of ion-ion and ion-neutral collisions based on trapping theory [e.g., *Hoppel and Frick*, 1986] correspond to the situation in which one partner is a molecular-sized ion. We have extended this scheme to derive physically consistent ion-ion recombination coefficients and ion-neutral collision kernels for clusters and particles of all sizes (from molecules to aerosols in the micron size range). In this new phenomenological description the trapping distance takes into account multiple collisions within the attractive potential sphere of the converging particles. The resulting coagulation kernels are natu-

rally pressure and temperature dependent. In the case of small-ion recombination these dependencies approach observed behavior. A detailed description of the methodology and comparison with available laboratory measurements will be presented in a separate manuscript.

The overall coagulation rate between charged particles is usually expressed in terms of an enhancement factor β that multiplies the equivalent neutral coagulation kernel. We adopt that convention here (refer to section 3.3.4), noting that for collisional processes involving at least one charged species, the accommodation coefficient (section 3.3.2) is taken as unity.

3.3.2. Accommodation coefficient. For our purposes, the accommodation coefficient α can be defined as the probability that a collision between two particles and/or molecular clusters, including monomers, leads to physical coalescence. Thus, for example, the average uptake of a vapor or cluster onto a surface, per collision, would be proportional to α (although the total vapor flux to the surface might be limited by other processes such as diffusion in the surrounding medium). The accommodation coefficient is sometimes ambiguously referred to as the sticking coefficient, which usually refers to chemically reactive uptake of a vapor. In our case, a distinction between these terms will not be made. In general, α is a function of the sizes, electrical charges, and compositions of the impinging particles.

The accommodation coefficient has a direct effect on the rate of coagulation in the "kinetic" regime, where at least one of the colliding particles has a mean free path longer than the dimensions of the larger particle. That is, the Knudsen number, $Kn=\lambda/r$, of the smaller particle (or vapor molecule) is >>1, where r is the radius of the larger particle and λ is the mean free path of the smaller. In this instance, the coagulation kernel is proportional to α. Otherwise, the smaller particle will tend to diffuse toward the larger one and be trapped in its vicinity by multiple collisions with the background gas.

At molecular scales the probability of association of two molecules or small clusters depends to a large degree on the binding forces within the collision complex and the efficiency of redistribution and thermalization of the internal energy of the excited complex. For simple molecules, few degrees of freedom are available and attractive van der Waals forces are weak. In this case, we may expect $\alpha<<1$. On the other hand, for small ions interacting with polar molecules the collision complex is almost always stabilized (for exothermic processes). Considering the size range of interest here, it is likely that the accommodation coefficient for neutral coagulation processes will increase rapidly from <<1 to ~1 as the cluster sizes increase [*Yu and Turco*, 1998].

For a given production rate of a precursor gas and surface area of the background aerosol, the concentration of free vapor is very sensitive to the molecular accommodation coefficient. In the case of H_2SO_4, a mean accommodation coefficient of 0.6 has been inferred from tropical field data [*Davis et al.*, 1999]. This value is adopted here as the maximum value, α_o, for the coagulation of H_2SO_4 molecules with uncharged clusters and aerosols of all sizes. Note that the effective value of α at very small sizes is much lower in our standard microphysical model (see below).

For all collisions that involve two oppositely charged clusters, the accommodation coefficient is taken as unity. Note that repulsion between species of the same sign of electrical charge is assumed here to preclude coagulation. The assumption of $\alpha=1$ for collisions that involve attractive Coulomb forces follows, in the case of small charged clusters, from a consideration of the limiting rates of ion-ion recombination. That is, ion-ion recombination is not generally limited by the sticking efficiency of the ions upon contact (since, as already pointed out, the collision complex in such cases is very stable). It is reasonable to extrapolate this behavior to larger charged clusters and particles.

When two molecules, or a molecule and small cluster, collide, the effective accommodation coefficient is likely to be significantly smaller than unity. This conclusion is consistent with laboratory measurements, in which collisionally stabilized molecule-molecule association reaction rate constants are typically found to be of the order of 10^{-12}–10^{-11} cm^3s^{-1}; that is, one to two orders of magnitude smaller than the collision kernel. This reduced efficiency may be explained in part by steric factors during the collision and by dissociation of the collision complex (see section 3.3.3). It is expected that α rapidly approaches unity as the clusters (or at least one of the collision partners) becomes larger than ~1 nm. Thus, as the van der Waals attractive forces at the interface increase [*Marlowe*, 1980a, 1980b], rebound of the clusters becomes less likely. The parameterizations used in this work to determine size-dependent accommodation coefficients are presented in section 3.3.4 following the discussion of cluster dissociation.

3.3.3. Evaporation/dissociation coefficient. In the present study, the loss of vapor by evaporation/dissociation, especially from small clusters, is addressed using an evaporation factor. Note that we need only consider the evaporation of monomers from clusters since, for the situations of interest, the evaporation of dimers is unlikely to be important. Evaporation is related to the equilibrium constant (thermodynamic stability) for a particular vapor-cluster interaction.

The equilibrium between a vapor and a cluster containing n condensed molecules of that vapor (where the cluster may be neutral or charged) is represented by

$$C_{n-1} + L \leftrightarrow C_n , \tag{1}$$

where L is the ligand, or condensing vapor molecule, and C_n is the concentration of clusters with n ligands. The equilibrium for this process is defined by

$$\frac{[C_n]_{eq}}{[C_{n-1}]_{eq}[L]} = K^o_{n-1,n}(T) = \frac{k_{f,n-1}}{k_{r,n}} . \tag{2}$$

The equilibrium constant K^o is a function of the Gibbs free energy change for the reaction, and is also equal to the quotient of the forward and reverse rate coefficients for (1). The rate of change in the concentration of the cluster, n, due to all processes involving monomers is given by

$$\frac{dC_n}{dt} = k_{f,n-1}[L]C_{n-1} + k_{r,n+1}C_{n+1} - k_{f,n}[L]C_n - k_{r,n}C_n . \tag{3}$$

Note that rate of loss of clusters of size n is controlled by a balance between association (condensation) and dissociation (evaporation), expressed by the last two terms in (3). The first two terms define the sources of these clusters (by growth and evaporation of clusters at adjacent sizes).

The set of relations (3) can always be solved using straightforward linear inversion techniques once the rate coefficients are defined. The forward rates are most accessible, being represented by the product of the collision kernel (with a charge enhancement factor if needed) and accommodation coefficient. The reverse rate coefficients can be calculated if the equilibrium constants (or thermodynamic free energies) of the clusters are known. For now,

we assume this is the case, and proceed to investigate the effect of evaporation.

Equation (3) can be cast in the form

$$\frac{dC_n}{dt} = -k_{f,n}[L]C_n\left[1+\frac{1}{[L]}\frac{k_{r,n}}{k_{f,n}}\right]+Q_n$$

$$= -k_{f,n}[L]C_n\left[1+\frac{k_{f,n-1}}{k_{f,n}}\frac{1}{[L]}\frac{1}{K^o_{n-1,n}}\right]+Q_n, \quad (4)$$

where Q_n is the cluster production rate. The term in brackets defines the total loss rate. We note that the equilibrium constant in (4) is equivalent to the equilibrium "vapor pressure" of the cluster (the equilibrium constant, nominally, has units of inverse concentration, or pressure). Indeed, one can define the cluster vapor pressure as

$$P^{(o)}_{L,n}(T) = RT/K^o_{n-1,n}(T) \ . \quad (5)$$

Since it is also known that the forward rate coefficients vary slowly with cluster number [*Castleman*, 1979], the ratio of forward rate coefficients in (4) will always be close to unity. Then we can write

$$\frac{dC_n}{dt} = -k_{f,n}[L]C_n\left[1+\frac{1}{S_{L,n}}\right]+Q_n \ , \quad (6)$$

where $S_{L,n}$ is the ligand vapor saturation ratio for cluster, n,

$$S_{L,n} = RT[L]/P^{(o)}_{L,n}(T) = [L]K^o_{n-1,n}(T) \ . \quad (7)$$

The equilibrium constant and the Gibbs free energy change depend on cluster properties. In the classical representation of a neutral cluster as an equivalent liquid droplet, it can be demonstrated that the vapor pressure defined in (5) is just the vapor pressure of the bulk condensate corrected for the Kelvin surface energy effect; in other words, the total vapor pressure of the droplet. Likewise, if the classical Thomson model is adopted for a charged cluster [*Castleman et al.*, 1978], the vapor pressure has a second correction term associated with the polarization energy of the embedded charge. Equation (7) is then seen to be the analog of the saturation ratio of a charged liquid droplet. In the thermodynamic representation the Gibbs free energy is described by the enthalpy and entropy changes for process (1). Nevertheless, the vapor pressure analogy in (7) remains valid.

From (6), we identify an evaporation coefficient as the empirical factor,

$$\varepsilon = \frac{S_{L,n}}{1+S_{L,n}} \ . \quad (8)$$

In effect, ε is the fractional probability that cluster n will grow under prevailing environmental conditions. In cases where the cluster vapor pressure is high (in other words, K^o is small, or k_r is large), S_L and ε will be small, and the clusters will be unstable. When the vapor pressure is low (that is, K^o is large, or k_r is small), S_L is large and ε approaches 1. In this situation the clusters grow freely. Typically, there will be a bottleneck to cluster growth where the vapor pressure is largest. This is equivalent to the free energy barrier for nucleation and marks the critical cluster size. Even if the vapor is supersaturated over very large clusters (droplets), $S_{L,\infty} > 1$, the saturation ratio over the critical cluster may still be small, $S_{L,n^*} << 1$. In general, S_L will be greater for a charged cluster compared to a neutral one of the same size and composition.

The evaporation coefficient ε depends on cluster size and charge, ambient temperature, the vapor pressure over the condensed ligands, and the presence in the cluster of potentially stabilizing species such as H_2O and NH_3. As a first approximation, the cluster free energies, vapor pressures, and evaporation coefficients may be calculated using the classical droplet model (or the Thomson model in the case of a charged cluster). The product of the evaporation and accommodation coefficients then defines a "net" accommodation coefficient, which represents the overall vapor condensation efficiency onto a cluster. In the case of water vapor uptake, it is reasonable to assume that each cluster instantaneously adjusts to an equilibrium state consistent with the local ambient relative humidity and temperature. Moreover, this state of quasi-equilibrium is maintained even as clusters gain or lose other ligands such as H_2SO_4 and NH_3, owing to the high concentration of water vapor in air, up to 1% or so. The previous analysis of evaporation still holds, except that the nth acid cluster, for example, must now be considered as a family of clusters, each consisting of n acid molecules but with varying numbers of water ligands defined by an equilibrium distribution, which varies with cluster size n. Averaging over the quasi steady-state water distribution yields appropriate mean rate coefficients for nth cluster kinetics. In the case of binary sulfuric acid and water mixtures, for example, the mean equilibrium weight percentage of acid in the cluster may be specified as a function cluster size [e.g., *Hamill et al.*, 1982].

Since little information is presently available to describe in detail the thermodynamic behavior of the specific clusters of interest, a simple adjustment to the accommodation coefficient is assumed as an expedient means of parameterizing these complex processes in the present work. It is reasonable to conclude, for example, that smaller clusters are less stable in general, and thus have a lower net growth rate. Moreover, clusters smaller than a critical embryo are more unstable than those larger than the critical size. Further, charged clusters are more stable than neutral ones. For the simulations discussed below, the accommodation coefficients have been modified to reflect these expectations, and measurements of limiting behavior have been employed to constrain the coefficients at small and large sizes.

3.3.4. Effective coagulation kernels. The parameterization of the coagulation kernels and net accommodation coefficients in the present APM model is illustrated in Figure 2. Data are provided in Figures 2a and 2b for collisions of vapor molecules (assumed to be hydrated H_2SO_4) with particles of all sizes, and in Figures 2c and 2d for collisions of particles of the same size. For these two cases the net accommodation coefficients α and coagulation enhancement factors β are shown in Figures 2a and 2c, while the resulting absolute coagulation kernels are given in Figures 2b and 2d, respectively. The curve marked 3 in Figure 2a is the mean accommodation coefficient for H_2SO_4 vapor condensation onto neutral particles as derived from observations [*Davis et al.*, 1999], for which we assume a value, $\alpha=\alpha_0=0.6$, as noted earlier. The corresponding curve 3 in Figure 2c is parameterized such that, while $\alpha=0.6$ for two monomers, it increases rapidly to unity as the sizes of the clusters increase. Using the curves 3 as a baseline, we then take cluster dissociation and steric factors into account in curves 5 (for neutral–neutral collisions). In this case, the radius of the critical embryo, which determines the transition from less stable to more stable clusters, is calculated using the classical droplet model, assuming the bulk properties of sulfuric acid/water

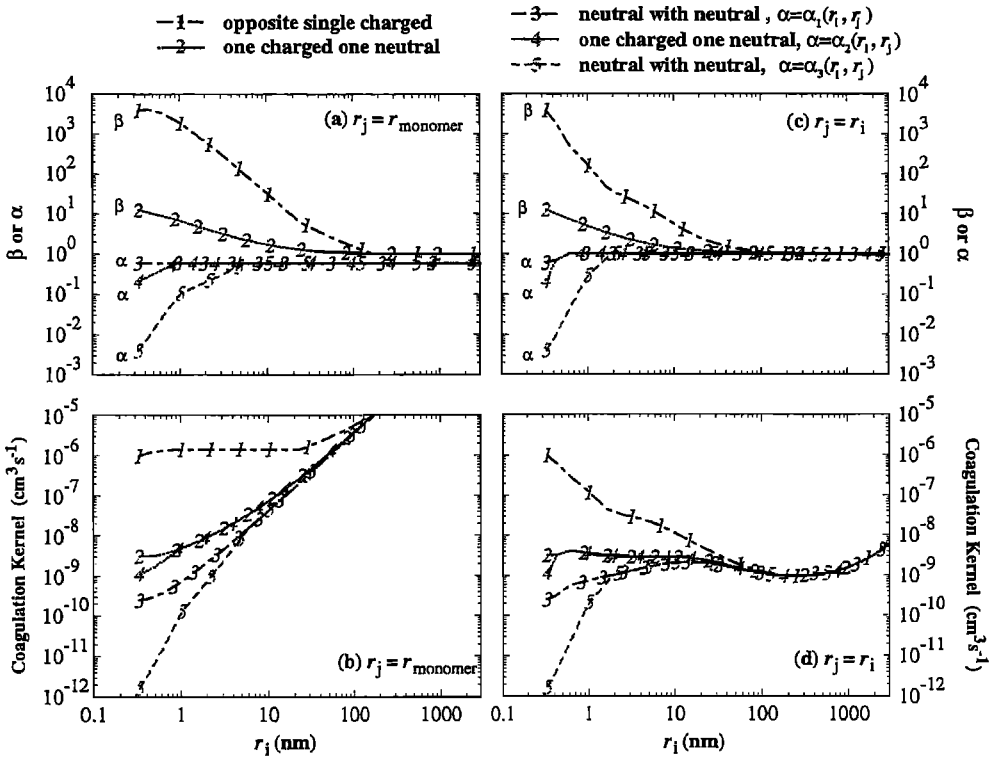

Figure 2. Dependence on size of (a, c) the coagulation enhancement factors β and net accommodation coefficients α for various combinations of particle size and charge, and considering possible cluster dissociation (refer to the legend); (b, d) the corresponding coagulation kernels. Figures 2a and 2b correspond to the coagulation of monomers with other particles spanning all sizes, while Figures 2c and 2d relate to the coagulation of two particles of the same size. Note in panel Figure 2a that for H_2SO_4 vapor condensation, the maximum accommodation coefficient is taken to be, α_c=0.6, and in case 2 the acid monomer is the neutral partner (see the text).

binary mixtures. The resulting critical size, and the net accommodation coefficients, are updated throughout a simulation as environmental conditions change (that is, curves 5 in Figure 2 are adjusted with regard to the points at which they converge with curves 3, using the results outlined in section 3.3.3).

The curve marked 1 in Figure 2a represents the enhancement factor β for the coagulation of a monomer ion with a charged particle of opposite sign, for all particle sizes. Likewise, curve 1 in Figure 2c gives β for two colliding ions of the same size and opposite electrical charge. The curves marked 2 in Figures 2a and 2c define the coagulation enhancement factors for collisions between a neutral and charged species (of either sign of charge) owing to the effect of image capture. In Figure 2a a neutral vapor molecule is assumed to impinge on a charged particle. Curves 4, which are similar to curves 3, take into account the possible dissociation of charged collision complexes smaller than the critical size (determined from the classical Thomson model). The net accommodation coefficients given by curves 4 multiply the enhancement factor curves 2. The corresponding coagulation kernels for charged species are shown as curves 1, 2, and 4 in Figures 2b and 2d.

The coagulation kernels for small charged clusters and molecules, as calculated here (Figure 2), are consistent with ion-neutral and ion-ion (opposite sign) reaction rate coefficients determined by laboratory experimentation. For example, the capture of a neutral polar H_2SO_4 molecule by a small charged cluster is predicted to be enhanced by a factor of ~10 over the equivalent neutral collision rate (that is, the collision kernel is ~10^{-9} cm^3s^{-1} as compared to ~10^{-10} cm^3s^{-1}, compare curves 2 and 3 in Figure 2b). Moreover, the predicted "ion-ion" recombination coefficient at molecular sizes (curve 1 in Figure 2b) is ~ 10^{-6} cm^3s^{-1}, which agrees with laboratory measurements and molecular theory at atmospheric pressures [*Loeb*, 1960].

At larger cluster sizes, electrostatic forces are much less effective. Polar molecules will still be attracted more strongly to charged particles than neutral ones, with significantly larger kernels at sizes up to several nanometers. When a charged cluster reaches ~10 nm in diameter, the advantage for vapor growth due to electrification becomes negligible (compare curves 2 and 3 in Figure 2b). Likewise, for equal sized particles the charged-neutral coagulation kernel at this point is also nearly identical to that for the equivalent uncharged particles (curves 2 and 3 in Figure 2d). For oppositely charged particles the coagulation (recombination) kernels actually fall off rapidly with increasing size (curve 1 in Figure 2d).

The predicted coagulation kernels corresponding to neutral-neutral association collisions involving very small clusters are likely to be considerably smaller than the kinetically limited values quoted above (i.e., ~10^{-10} cm^3s^{-1}). For example, curves 5 in Figures 2a and 2c, at the molecular scale, yield molecule-molecule association reaction rate constants that are consistent with typical experimental values, ~10^{-12} cm^3s^{-1}. In this context the curves marked 3 in Figure 2 probably represent the maximum kernels for neutral species in our model. At nanometer sizes, there is some evidence that collision kernels are enhanced by van der Waals attractive forces, although these are quite weak [*Marlowe*,

1980a, 1980b; *Alam*, 1987]. The van der Waals effect is likely to express itself through an increase in the net accommodation coefficient rather than an enhancement in the collision cross section, since the forces are of such short range. We carry out sensitive tests below using curves 3 and 5, showing that recent field data on H_2SO_4 concentrations are, in fact, consistent with accommodation coefficients significantly lower than those given by curve 3.

The size-dependent behavior of the absolute coagulation kernels and electrostatic enhancement factors (Figure 2) has several important consequences. First, the growth rates of ionized clusters, especially at small sizes, can be enhanced by an order of magnitude over those of equivalent neutral species. Accordingly, for a given concentration of a precursor, ions are more likely to achieve stable dimensions. Second, the scavenging of ion clusters by preexisting aerosols prior to reaching observable sizes rapidly becomes more improbable as the precursor concentration increases. Finally, since the neutral clusters that result from the recombination of charged clusters will be larger than the clusters that arise spontaneously from the vapor, aerosols initially condensing around ions are likely to retain a growth advantage for a period extending beyond neutralization.

4. Marine Boundary Layer Ultrafine Particle Bursts

4.1. Assessing Field Data from PEM

The modeling approach just described is applied to a case study involving ultrafine aerosol production in the marine boundary layer during the Pacific Exploratory Mission (PEM) Tropic-A field project. To simplify matters, the particles are assumed to be composed exclusively of H_2SO_4-H_2O mixtures (with the amount of condensed water determined by equilibrium at the local relative humidity). While other species (e.g., NH_3, HNO_3, etc.) may also contribute to the initial growth and stability of the smaller clusters and particles, their contribution to the total ultrafine aerosol abundance is not likely to be a dominant factor under the circumstances encountered. For example, while ammonia could lead to greater cluster stabilization, if it were present, ammonia alone is unlikely to modify the overall aerosol growth rate significantly (see below, and the section following). Nitric acid has relatively small concentrations in the clean marine environment, and has not been implicated in ultrafine aerosol nucleation. Accordingly, at least in the early stages of particle formation, sulfuric acid appears to be the controlling condensate.

During PEM Tropic-A, simultaneous measurements were obtained of key gas-phase species as well as ultrafine aerosols in different size ranges [*Clarke et al.*, 1998]. In one particular flight, aircraft-based measurements were obtained over a horizontal distance of 360 km at a height of ~160 m above the ocean surface during the period 1330–1430 (LT). These data reveal regions identified as having no detectable nucleation, the onset of nucleation, ongoing active nucleation, aging nucleation, and aged nucleation [*Clarke et al.*, 1998]. A notable burst of particle formation was detected in an air mass that had experienced recent precipitation scavenging, retaining a high relative humidity (RH~95%) and low background particle surface area density (~7 $\mu m^2 cm^{-3}$).

To investigate this event in the context of ion-mediated nucleation, we initialized an APM simulation at 1100 LT using the observed values of T=298.25 K, RH=95%, and wet aerosol surface area density of 7 $\mu m^2 cm^{-3}$. The background aerosols in this case include an accumulation mode and a sea-salt mode, as is normally seen in the tropics (refer to Figure 3 for the initial size distribution). The temperature and humidity were held constant over the course of the model calculation, while the aerosols at all sizes evolved microphysically (although the initial ambient particles changed very little; refer to Fig. 4c). At time zero we also assumed that the concentration of sulfuric acid vapor was 10^6 cm^{-3}, the ambient ion concentration (positive or negative) was 500 cm^{-3}, and the ionization rate was 2 ion-pairs $cm^{-3}s^{-1}$ (and remained constant over time). Of these latter parameters the initial H_2SO_4 concentration is least important, inasmuch as photochemical production and condensation dominate the H_2SO_4 abundance after several minutes. Accordingly, for the present simulations, the H_2SO_4 production rate was parameterized as

$$d[H_2SO_4]/dt = a \sin\left[\frac{\pi}{12}(t-6)\right] \quad (6 < t < 18\ hrs)\ . \qquad (9)$$

Here $a=10^4$ $cm^{-3}s^{-1}$, as determined by *Clarke et al.* [1998] from simultaneous measurements of sulfur dioxide and OH concentrations. Finally, the coagulation kernels for oppositely charged clusters/particles were adopted from the curves marked 1 in Figure 2b and 2d, for neutral–charged particle interactions, from curves 4, and for neutral-neutral interactions, from curves 5.

Figure 3 illustrates the predicted evolution of the concentrations of H_2SO_4 vapor and total ultrafine condensation nuclei (UCN) having d>3 nm, along with the ratio of condensation nuclei (CN) having d>10 nm to UCN (the CN/UCN ratio). The 4-hour simulation follows the history of a single air mass initialized at 1100 LT in very clean air and presumably encountered by the aircraft at a series of later times (with "sampling" of the air mass occurring continuously over the course of the simulation). In reality, the measurements occurred during a single pass of the aircraft through a region assumed to have relatively homogeneous properties. In other words, to make comparisons between the model predictions and field observations, temporal variations sensed by the airborne instruments are taken to represent the mean evolution of the larger air mass experiencing particle formation. Bars to the right side of Figure 3 indicate the ranges of the H_2SO_4, UCN, and CN/UCN measurements collected during a 1-hour sampling period corresponding to the penetration of the nucleation zone.

The simulations suggest that H_2SO_4 vapor recovers quickly in the cloud-processed air mass to ~10^7 cm^{-3} (within 16 min), reaching a peak concentration of ~3×10^7 cm^{-3} some 80 min after precipitation scavenging. Thereafter, H_2SO_4 decreases steadily and approaches 1.5×10^7 cm^{-3} at 1400 LT, due to vapor uptake on newly formed particles and the decrease in sulfuric acid production as OH and SO_2 concentrations drop in the air mass. We note that expected changes in the relative humidity, which were not included, would have little effect on the outcome of the simulation. Within ~30 min of the precipitation event that scoured the air mass, a significant number of newly formed UCN appear (note the sudden decrease in the CN/UCN ratio at this time). By 12:15, the total UCN concentration approaches 10^4 cm^{-3}, eventually growing to ~2.0×10^4 cm^{-3} at 14:00. The CN/UCN ratio is very low (<0.1) just as nucleation begins, but quickly rises to >0.6 at 14:00 as the freshly formed particles age. It is noteworthy that, for the PEM experiment, classical binary homogeneous nucleation theory would have predicted negligible particle formation.

The maximum concentration of H_2SO_4 simulated here (~3×10^7 cm^{-3}) is somewhat less than the extreme observation (~5×10^7 cm^{-3}). This may indicate that the production rate of H_2SO_4 was greater in certain regions of the nucleation zone, that the air was

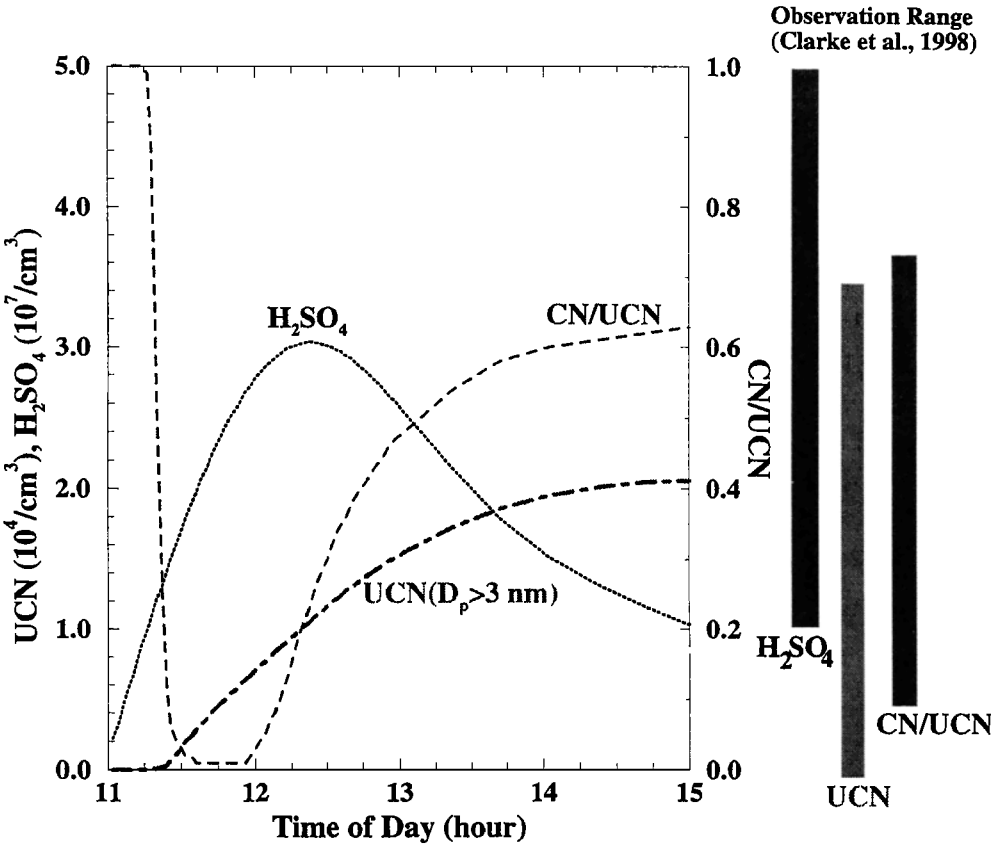

Figure 3. Simulated evolution of H_2SO_4 vapor concentrations, total ultrafine CN (UCN; d>3 nm) number densities, and CN/UCN ratios in a marine boundary layer air mass recently scavenged by precipitation. The bars at the right edge of the diagram show the ranges of the observations [*Clarke et al.*, 1998] during a 1-hour flight in NASA's PEM Tropic-A campaign.

initially cleaner in places, that the overall accommodation coefficient for H_2SO_4 vapor on particles was somewhat lower, or that other factors contributed to the compositional variability. For the peak H_2SO_4 recorded, the maximum observed UCN concentrations of ~3×10^4 cm^{-3} would be consistent with theoretical expectations (that is, UCN concentrations >2.0×10^4 cm^{-3} would be predicted in correspondence with higher levels of H_2SO_4). A greater ionization rate or initial ion concentration would also increase the number of UCN calculated by the model. Since the air mass had recently been processed by a precipitating cloud system, it is plausible that the charge level may have been enhanced by cloud electrification processes, although we have no other evidence for this effect.

Figure 4 shows, for the simulation depicted in Figure 3, the evolution of the size distributions of the total charged (positive + negative) particles (Figure 4a), the neutral particles (Figure 4b), and the total particle population (charged + neutral) (Figure 4c). The preexisting background particles, which are assumed to be neutral initially, rapidly attract ambient small ions and establish an equilibrium charge distribution (within 10 min). In the APM model the initial, and any newly generated, H_2SO_4 molecules, positive ions, and negative ions, are always placed in the first size bin of the neutral, positively charged, and negatively charged particle types, respectively. We do not consider in any detail the ion reactions leading up to the initial stable core ions (hydrated bisulfate and hydronium among others, which are always inserted into the first dry model bins; refer to section 3.2). Likewise, we do not explicitly treat the interactions of ions with other gaseous species such as HNO_3 and NH_3. As mentioned previously, subsequent growth of the charged particles is assumed to be limited by sulfuric acid uptake.

Clearly depicted in all of the panels in Figure 4 is the growth and accumulation of pre-nucleation clusters and nanoparticles as the concentration of H_2SO_4 increases after precipitation scavenging (as in Figure 3). At 10 min into the simulation most of the clusters are still below the critical neutral size, ~1.8 nm diameter. We estimate the critical embryo size using the standard droplet model for a binary liquid, since no other information is available. Hence the critical size will vary with the H_2SO_4 vapor concentration, as well as humidity and temperature. The high relative humidity in the PEM case implies a critical cluster of roughly 5-10 sulfuric acid molecules, significantly fewer than at lower humidity. For ease of calculations we take the same critical size for both the neutral and charged clusters. The greater inherent stability of the charged clusters is approximated in terms of the net accommodation coefficient, as discussed in section 3.3.4.

By 30 min, a significant number of the clusters have achieved supercriticality, even reaching nanometer dimensions. Importantly most of these "nucleated" nanoparticles began as electrically charged clusters, with the advantage of accelerated growth due to electrostatic effects. The neutral clusters, on the other hand, grow more slowly and fail to exceed the critical size by a significant factor under the prevailing conditions. The mode of neutral ultrafine particles that appears after ~30 min in Figure 4b

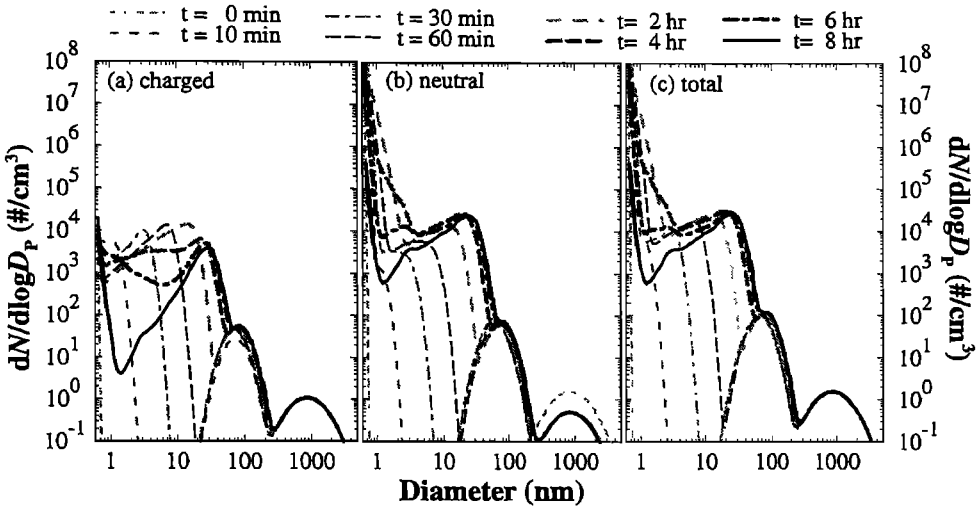

Figure 4. Simulated evolution of the size distributions of (a) charged particles (positive plus negative), (b) neutral particles, and (c) total particles. The results correspond to the case shown in Figure 3. The observed background aerosols are represented by the two largest modes of the size distribution.

is due to the neutralization of charged nanoparticles by small ions. After 1 hour, a distinct nucleation mode (with mean diameter of ~7 nm) is apparent; this mode is clearly associated with the ionized clusters. As the air mass continues to age, and additional H_2SO_4 is generated, more clusters are activated and accumulate in the nucleation mode. At the same time, the new particles continue to grow, and reach a mean diameter of ~20 nm after 4 hours or so. Most of the charged clusters and particles below ~20 nm in Figure 4a consist of primary ions originally produced by galactic cosmic radiation. The fraction of secondary ions created by charge uptake onto neutral particles is very small in this size range. As the charged particles grow, however, their neutralization rate (by small ions of opposite sign) increases. Consequently, most of nucleation mode particles are electrically neutral after 4 hours.

During their evolution from small clusters to nanoparticles a fraction of the putative aerosols are scavenged by preexisting (background) particles, as well as those recently nucleated. Hence the resulting ultrafine aerosol concentration is a balance mainly between vapor nucleation and cluster scavenging. After 4 hours the production rate of new supercritical clusters is significantly reduced, owing to a decrease in H_2SO_4 vapor associated with a reduction in its photochemical production rate, along with an increase in particle surface area. Subsequently, the concentrations of clusters and particles smaller than 10 nm perceptibly decline as a consequence of scavenging.

4.2. Homogeneous Particle Formation: An Alternative Hypothesis

It is apparent that species in addition to H_2SO_4 and H_2O can play a role in aerosol formation and growth [e.g., *Turco et al.*, 1998; *Kulmala et al.*, 2000]. In particular, ammonia and organic compounds are likely to react with, and stabilize, acidic clusters.

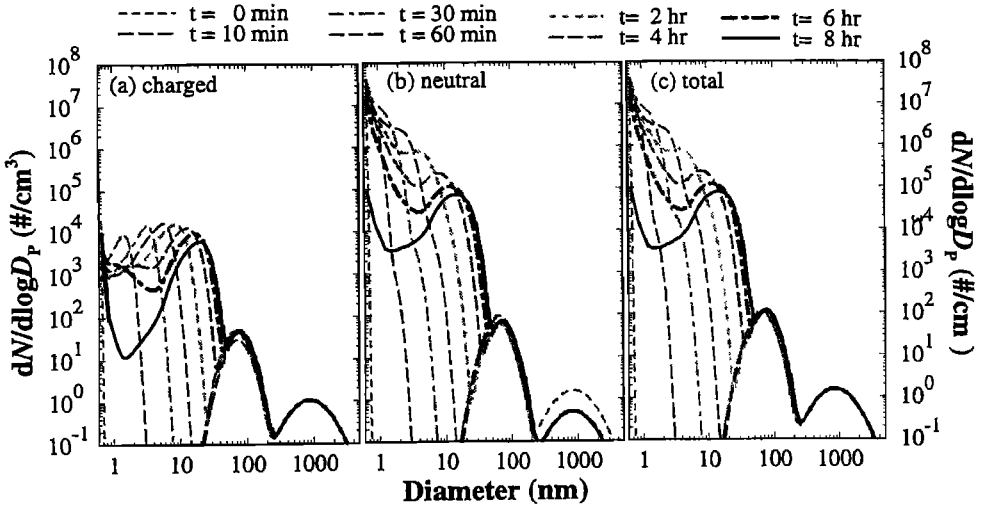

Figure 5. Same as Figure 4, except that the maximum accommodation coefficients for neutral-neutral collisions (i.e., the curves marked 3 in Figure 2) are used in the simulation.

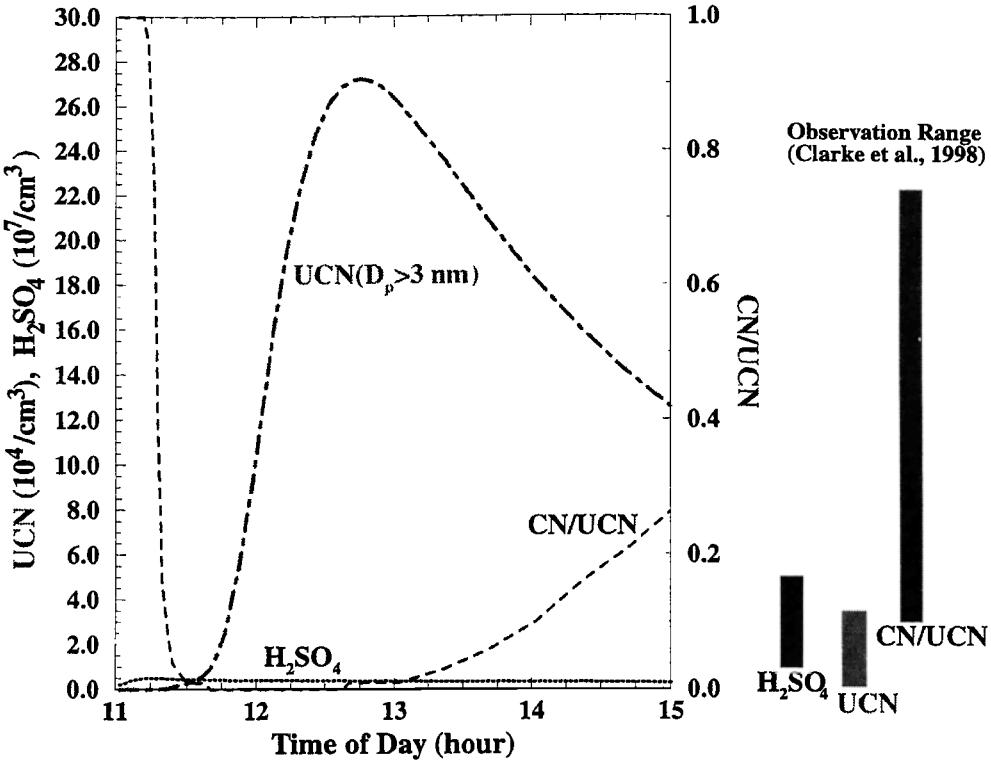

Figure 6. Same as Figure 3 except, as in Figure 5, the maximum accommodation coefficients for neutral-neutral collisions (i.e., the curves marked 3 in Figure 2) are employed.

In the formulation of section 3, this would lead to a lowering of the cluster vapor pressure and evaporation rate. In the extreme case, which is unlikely to occur in the lower atmosphere, the cluster vapor saturation ratio becomes large at all sizes. The evaporation coefficient then approaches unity, and the net accommodation coefficient becomes α_o (section 3.3.4).

In Figures 5 and 6, results are presented for an extreme case in which the accommodation coefficients for neutral vapor-cluster and cluster-cluster interactions are effectively maximized (i.e., the curves marked 3 in Figures 2a and 2c, rather than curves 5, used in the calculations of Section 4.1). All the other parameters are similar. This case study represents the fastest particle growth scenario and the most competitive situation for homogeneous nucleation (i.e., with perfect sticking and the absence of a nucleation barrier). As we can see from the size distributions shown in Figure 5, while the charged clusters retain their growth advantage, neutral vapor coagulation has become quite efficient because of the high concentration of uncharged molecular clusters. Indeed, the neutral particle mode eventually overtakes the ion-nucleation mode at late times (i.e., the ion nucleation mode is subsumed within the neutral mode). However, the predictions for this case are inconsistent with observations in several regards, as can readily be seen in Figure 6. First, the calculated number of UCN particles approaches a maximum value of 2.7×10^5 cm^{-3} at ~1245 LT, which is roughly an order of magnitude greater than the highest measured concentration. Second, the maximum abundance of H_2SO_4 in the model peaks near 6×10^6 cm^{-3}, which is much lower than the observed concentrations. Finally, the CN/UCN concentration ratio is also inconsistent with the field data. In other words, the simulation fails to explain the observations in almost every respect.

Because of the assumption of efficient accommodation for neutral-neutral collisions in this case study, the H_2SO_4 vapor abundance is found to be strongly suppressed, preventing concentrations from reaching ~10^7 cm^{-3}. Hence we can infer that the accommodation coefficients for collisions between neutral molecules and small clusters must be significantly smaller than unity, as proposed in section 3.3. Indeed, lower accommodation coefficients, like those used for the simulations illustrated in Figures 3 and 4, turn out to be consistent with a variety of measurements in the boundary layer [*Yu and Turco*, 2000a] and in aircraft plumes [*Yu and Turco*, 1998], as well as recent ab initio molecular interaction calculations [*Ianni and Bandy*, 2000].

5. Galactic Cosmic Ray Modulation: Impact on Aerosol Formation

5.1. Correlation of GCR Fluxes With Changes in Cloud Properties

Recently, satellite observations of Earth have been interpreted to show that variations in global cloud cover are correlated with changes in the flux of galactic cosmic rays (GCRs) entering the atmosphere [*Svensmark and Friis-Christensen*, 1997; *Svensmark*, 1998]. Since the GCR intensity varies inversely with solar activity, changes in cloud cover would therefore be correlated with the 11-year solar cycle. *Svensmark and Friis-Christensen* [1997; also *Svensmark*, 1998] deduce a variation in cloud coverage of up to ~3-4% corresponding to changes in galactic cosmic ray intensities of up to 20% over the 11-year cycle. More recent work shows that this correlation applies mainly to low clouds [*Marsh and Svensmark*, 2000]. The microphysical properties of the clouds that

contribute to this inferred behavior were not determined. However, since clouds play a key role in the radiation balance, any significant solar influence on global cloud properties has the potential to impact climate [e.g., *Svensmark*, 1998]. In this context, it is crucial to identify potential microphysical mechanisms that may link solar activity with cloud cover or opacity.

A number of studies [e.g., *Pudovkin and Veretenenko*, 1995; *Menzel et al.*, 1997; *Feynman and Ruzmaikin*, 1999; *Soon et al.*, 2000] have suggested linkages between GCR fluxes and global cloudiness, or climate change more generally [see *Tinsley*, 1996; *Soon et al.*, 2000]. *Pudovkin and Veretenenko* [1995] deduced a correlation between short-term decreases in cloud cover at higher latitudes and sudden Forbush decreases in GCRs. This effect appeared to be associated primarily with high-level cirrus clouds, however. *Feynman and Ruzmaikin* [1999] recently proposed that longer-term increases in global tropospheric temperatures (over the last century) were correlated with an increase (by 25%) in the high-latitude area subject to the most intense GCR irradiation. *Soon et al.* [2000] also presented data supporting a relationship between the area of the solar coronal hole, which is locked to the 11-year solar cycle and thus is related to GCR influx, and the mean temperature of the lower troposphere over a 20-year period. They suggested that the correlation could have a number of interpretations aside from the GCR-flux/cloud-cover link, however, including solar charged-particle influences on the upper atmosphere, ozone layer perturbations [*Shindell et al.*, 1999], or perhaps other solar terrestrial coupling mechanisms.

Kernthaler et al. [1999] extended the approach of *Svensmark and Friis-Christensen* [1997] by looking into the different cloud types (high, midlevel, and low), and found no clear relationship between cosmic ray flux and individual cloud types. *Kernthaler et al.* [1999] also pointed out that the amplitude of the total cloudiness variation in phase with GCR flux seen in ISCCP data is reduced (from ~3-4% to ~2%) if high latitude data are included in the analysis. However, *Svensmark and Friis-Christensen* [2000] pointed out that the catalog of individual cloud types in the ISCCP-C2 data set used by *Kernthaler et al.* [1999] is unreliable and has been replaced in ISCCP-D2 by data derived from an improved cloud algorithm. The results of *Kernthaler et al.* [1999] cannot be reproduced with the revised ISCCP-D2 data set, which shows a high correlation between GCR variations and low cloud cover change [*Marsh and Svensmark*, 2000]. On the other hand, *Kuang et al.* [1998] had found that the changes in cloud coverage inferred by *Svensmark and Friis-Christensen* [1997] were almost exactly offset by compensating variations in cloud opacity, and raised the possibility that the overall changes were small, and associated with the concurrent El Nino cycle. *Soon et al.* [2000], in their review of the relevant information, rebutted some of *Kernthaler et al.*'s [1999] criticisms regarding previous interpretations of cloud observations, nevertheless concluding that the existing data are insufficient to establish a GCR/cloud connection.

Given these conflicting interpretations of apparent solar cycle and GCR correlations with cloud properties, it is even more urgent to identify possible linking mechanisms. Toward that end, we adopt the hypothesis that variations in the rate of ion production by galactic cosmic rays can modulate the number of atmospheric condensation nuclei, and seek to quantify that relationship. The subsequent evolution of the CN into cloud condensation nuclei involves numerous additional factors, including much longer timescales and a variety of trace species. Hence that more extensive sensitivity analysis will be left for future work.

5.2. Simulations of the Consequences of GCR Variations

In section 4, it was demonstrated that background ionization is intimately involved in the formation of ultrafine (volatile) aerosols in the lower troposphere, and is capable of explaining a number of observations in this regard. Moreover, the ion mediated nucleation (IMN) mechanism [*Yu and Turco*, 2000a] acts ubiquitously, occurring whenever aerosol precursors are present in sufficient quantities. It is therefore logical to investigate the variations in aerosol properties associated with the modulation of ambient ionization levels as a result of solar cycle forcing of the GCR intensity. In particular, we wish to calculate the variations in CN concentrations associated with changes in cosmic ray fluxes, inasmuch as this represents the second step in the phase change leading from vapor to CCN (the first step consisting of molecular aggregation around ion cores).

For these simulations, conditions identical to those in section 4 are adopted. Therefore the model calculations conform to the results presented in Figures 3 and 4. The only parameter that is varied in this case is the ionization rate (Q), which is taken to range from 2 to 2.5 ion-pairs $cm^{-3}s^{-1}$ (i.e., a 25% increase above the baseline value employed earlier). This change is roughly consistent with the maximum relative variation in the GCR flux expected over the course of a solar cycle. Hence it is also the variation in ionization rates that would be predicted for the marine boundary layer over the course of time.

Figure 7 shows the predicted evolution of the total concentration of condensation nuclei $N_{d>d_i}$ (d_i =3, 10 and 30 nm). Figure 7a gives the absolute concentrations, while Figure 7b shows the relative changes in the total concentration. The simulations indicate that a 25% increase in the ionization rate (from 2 to 2.5 ion-pairs $cm^{-3}s^{-1}$) results in a maximum 16.5% increase in ultrafine CN (UCN; d>3 nm) and 9% increase in CN (d>10 nm) several hours after nucleation is initiated. However, this maximum perturbation decays over time due to subsequent loss of the CN by self-coagulation and scavenging by preexisting aerosols. After about 8 hours, the CN perturbation is still ~7–8%. Most of newly formed particles remain smaller than 30 nm at this time (refer to Figure 4), and the perturbation in particles larger than 30 nm is negligible (Figure 7).

In order to influence cloud properties some of these newly formed ultrafine particles must grow and eventually contribute to the CCN population (d>~80 nm). Under any circumstances the formation of new CN will eventually contribute to background CCN. However, the fraction of CCN originating from ionization connected with galactic cosmic radiation, versus other direct and indirect aerosol sources, depends on location, altitude, season, and other factors. Direct sources of CCN include biomass combustion, sea salt and dust suspension, and various anthropogenic emissions. Such particles may also form in association with ionization from natural radioactive decay, lightning, corona discharge, and combustion, as well as homogeneous nucleation processes.

The GCR CN source (as in Figure 7a) is subject to ongoing depletion by self-coagulation, deposition, scavenging on preexisting aerosol surfaces, cloud processing, and air mass dilution (e.g., see *Yu and Turco* [1999], where the long-term evolution of aircraft aerosols is simulated under analogous circumstances). Accordingly, the growth rates of the freshly nucleated CN particles over a period of hours to days will have a strong influence on the number that survive to become CCN. It may be deduced from Figure 7b that if condensates other than sulfuric acid were avail-

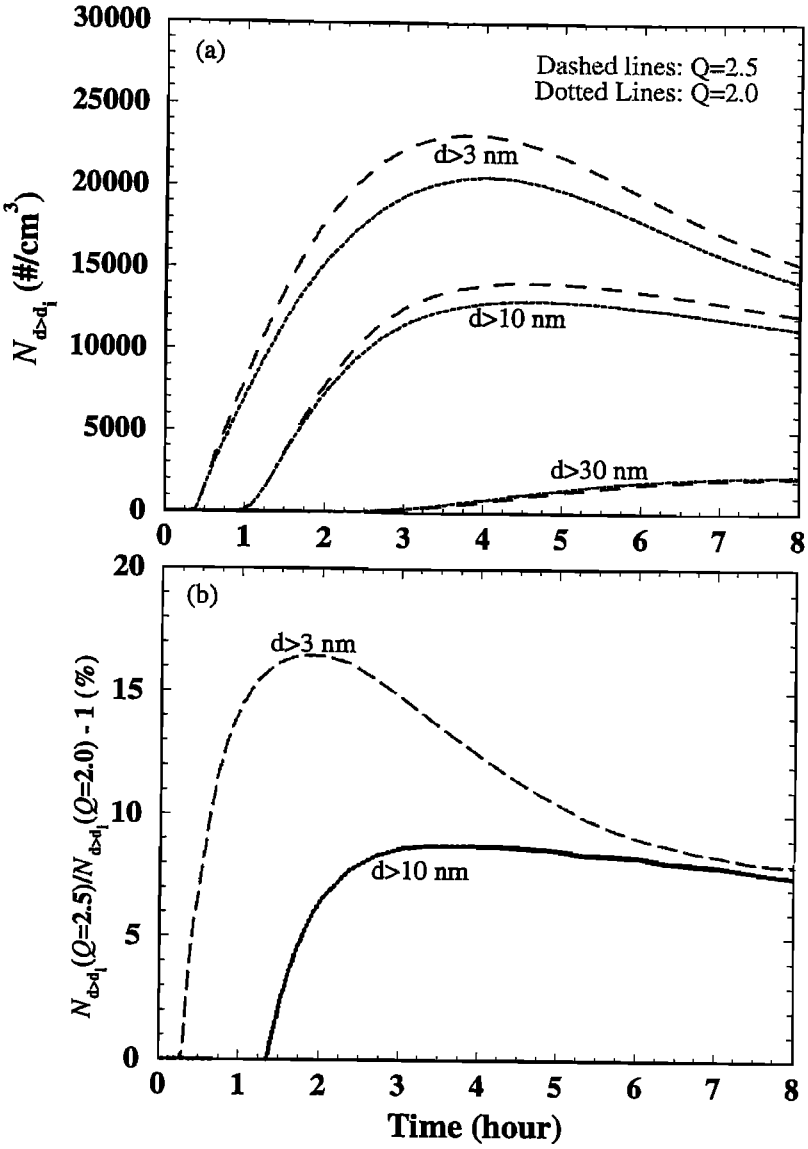

Figure 7. Predicted differences in the total concentrations of condensation nuclei $N_{d>d_i}$ (d_i=3, 10 and 30 nm), for two different assumed GCR ionization rates (Q=2.0 and 2.5 ion-pairs cm^{-3}s^{-1}). All other parameters conform to the case shown in Figures 3 and 4. (a) Absolute particle concentrations for d_i=3, 10, and 30 nm; (b) Relative fractional changes (in percent) in the integrated concentrations (i.e., $F = N_{d>d_i}(Q=2.5)/N_{d>d_i}(Q=2.0) - 1$).

able in high enough concentrations in the vicinity of a nucleation event, the CCN population could conceivably increase by 10-15% or more (assuming GCR-induced ion-mediated nucleation is the dominant source of new particles, and that 3-nm particles can grow to ~80 nm prior to scavenging [e.g., *Yu and Turco*, 1999]). It follows that a wide range of uncertain and variable parameters can influence the formation rate and growth of GCR-induced CN and CCN, including H_2SO_4 and NH_3 concentrations, background particle surface areas, temperature, relative humidity, and the presence of additional condensable compounds, especially organic vapors.

The impact of changes in the ionization rate on particle production is greatest when the rate is relatively low, the preexisting aerosol surface area is low, and the H_2SO_4 concentration is high. Under these circumstances, ionization rates are the limiting factor in particle nucleation. This is the case for marine boundary layer air masses recently subject to precipitation scavenging, as simulated here. If the ionization rate were greater (as in the upper troposphere and stratosphere), and the H_2SO_4 concentration more modest, the sensitivity of particle formation to the ionization rate would be weaker (H_2SO_4 would become the limiting factor under these circumstances). In addition, whenever the background aerosol surface area is elevated, nucleation is strongly inhibited and CN concentrations are only weakly dependent on the ionization rate. It has been suggested that galactic cosmic rays cannot have a significant impact on the stratospheric aerosol population [*Mohnen*,1990].

The ionization rate affects the fractions of CN and CCN that are charged at any time. In the IMN mechanism, these fractions are calculated explicitly, since the uptake of charge on larger particles can control the abundances of small ions and suppress the ion nucleation rate. *Tinsley* et al. [2000] have suggested that electrostatic charge accumulating on supercooled water droplets and aerosols may affect the rates of ice nucleation, and sedimen-

tation of ice crystals in precipitating clouds, particularly in the middle troposphere. Charged particles may also experience differential scavenging rates [e.g., *Tammet and Israelsson*, 1999] and chemical reactivities (vapor uptake coefficients [*Aikin and Pesnell*, 1998]). It follows that any link between solar activity and Earth's climate through the modulation of GCR fluxes and ionization rates would likely involve complex physical and chemical mechanisms, in which aerosols are implicated.

In order to quantify the effect of GCR variations on CCN populations, longer-term simulations are required since it typically requires several days for nucleated particles to grow into the CCN size range. In such cases, other physical processes, especially aerosol–cloud interactions, must be carefully considered. Importantly, the contribution to particle evolution associated with the condensation of species other than sulfuric acid remains to be quantified.

5.3. Expected Relationship of GCR Variations to Aerosol Population

The expected dependence of aerosol concentrations on the local ionization rate can be estimated using (3) if a recombination term is added (and cluster dissociation is neglected). Then, for the nth cluster,

$$\frac{dC_n}{dt} = k_{f,n-1}[L]C_{n-1} - k_{f,n}[L]C_n - C_n/\tau_{rn}\,, \tag{10}$$

while for the first clustering step,

$$\frac{dC_0}{dt} = Q - k_{f0}[L]C_0 - C_0/\tau_{r0}\,. \tag{11}$$

Here Q is the ambient ionization rate (due to GCRs in this case), and the charged cluster lifetime against recombination, τ_{rn}, is defined in terms of the ion-ion recombination coefficient, k_{rn} (cm^3s^{-1}) and total ion concentration, n_{io}, as,

$$\frac{1}{\tau_{rn}} = k_{rn}n_{io}\,; \quad n_{io} \equiv \sqrt{Q/k_r}\,. \tag{12}$$

In (12), n_{io} is estimated as the quasi steady state concentration corresponding to the mean recombination coefficient for the cluster distribution.

Under quasi steady state conditions, the series of (10) through (12) can be solved to yield the flux of particles growing from size n to the next larger size; i.e., I_n (number $cm^{-3}s^{-1}$). Assuming that the values of k_f, k_r, and τ_r are the same for all of the clusters of interest (a reasonable approximation at this point), the flux is derived as

$$I_n = Q\left(\frac{1}{1+\sqrt{Q}\sqrt{k_r}/k_f[L]}\right)^{n+1} = Q\left(\frac{1}{1+\tau_g/\tau_r}\right)^{n+1} \tag{13}$$

where the time constants for cluster neutralization and growth are defined by

$$\frac{1}{\tau_r} = \sqrt{Qk_r}\,; \quad \frac{1}{\tau_g} = k_f[L]\,. \tag{14}$$

We note that the flux in (13) can be a strong function of the ionization rate when the ion neutralization time constant τ_r is shorter than the clustering time constant τ_g,

$$I_n \approx Q^{-(n-1)/2}[L]^{n+1}\left(k_f/\sqrt{k_r}\right)^{n+1}\,. \tag{15}$$

This follows because the ion clusters do not have sufficient time to reach the larger sizes prior to recombination (and thus presumably, dissociation). Obviously, whenever ion growth is restricted, the particle nucleation rate will be extremely sensitive to the GCR flux, while the nucleation rate will be very small.

On the other hand, if $\tau_g \ll \tau_r$ (or, $[L] \gg \sqrt{Q}\times 10^6$ cm^{-3} assuming typical values of k_f and k_r, and with Q in units of ion-pairs $cm^{-3}s^{-1}$), (13) becomes

$$I_n \approx Q\left(1-\frac{\sqrt{Q}\sqrt{k_r}}{k_f[L]}\right)^{n+1}$$

$$\approx Q\left[1-(n+1)\frac{\sqrt{Q}\sqrt{k_r}}{k_f[L]}+\frac{n(n+1)}{2}\left(\frac{\sqrt{Q}\sqrt{k_r}}{k_f[L]}\right)^2\right]. \tag{16}$$

Under these conditions, I_n is roughly proportional to Q^c with $c \lesssim 1$ and the value of c depends on τ_g/τ_r.

If there is a "critical" sized charged embryo, n^*, above which the neutralized clusters are stable, then the particle formation rate, or nucleation rate, is given by I_{n^*}. The flux in (13), (15), and (16) represents the local instantaneous quasi steady state particle production rate. Hence the change in the total number of particles in an air mass is the time integral of this rate (ignoring for the moment aerosol losses by other processes). In the present case the growth of the ion clusters is rapid enough to overcome the limitations of recombination (at least, once the abundance of H_2SO_4 exceeds ~3×10^6 cm^{-3}). One might expect the change in concentration, for short periods, to be roughly proportional to Q^c based on the previous analysis.

It also follows that the change in the local particle population over longer periods will be sensitive to the ionization rate in a more complex way. The model simulations in Figure 7, in fact, reveal a much lower sensitivity; roughly $Q^{1/3}-Q^{1/4}$ after the time interval shown (t=8 hours), for a relatively small change in Q of 25%. The reduced response follows because the system of ions, particles, and vapors is considerably more rigid than (10) represents. Indeed, a number of interactions between the components of this system, some of which were mentioned earlier and are not included in (10), act to stabilize the particle population. Such systemic nonlinear interactions were represented in a simplified way by *Turco et al.* [2000], who obtained analytical solutions in certain limiting cases applicable to the marine boundary layer. As derived by *Turco et al.* [2000], the dependence of the asymptotic aerosol concentration on the background ionization rate varies in proportion to $Q^{1/3}-Q^{1/6}$ (for critical cluster sizes ranging from 3 to 9 sulfuric acid molecules). This dependence is consistent with the present numerical predictions. In fact, for the weakest dependence found by *Turco et al.* [2000] a 25% change in GCR irradiation implies roughly a 4% change in the stable aerosol population, after accounting for feedback effects. While this result is similar to the cloud cover variation identified by *Svensmark and Friis-Christensen* [1997], no physical connection between GCRs and cloudiness can be solidly inferred from the present analysis.

6. Summary

We have described a comprehensive "kinetic" approach for studying aerosol formation under atmospheric conditions. A unified kinetic collision mechanism is derived that simulates the buildup of charged and neutral molecular clusters, and their

growth into nanoparticles. This approach allows the effects of ionization on cluster growth and nucleation to be explicitly formulated. We find that charged clusters formed on air ions are more stable and can grow faster than corresponding neutral clusters. The enhanced growth and stability, a consequence of electrostatic interactions, provides a key competitive advantage to electrically charged embryos. An ion-mediated nucleation (IMN) mechanism that accounts for such processes was previously designed and applied to explain the observed formation of ultrafine particles at a remote continental site, as well as the diurnal variation of the mobility spectrum in the lower atmosphere [*Yu and Turco*, 2000a].

In the present work, IMN theory has been applied to study the role of ubiquitous galactic cosmic ray (GCR) ionization in marine boundary layer (MBL) aerosol formation. Simulations are used to explain a major nucleation event recorded during NASA's Pacific Exploratory Mission (PEM) Tropic A [*Clarke et al.*, 1998]. It is concluded here that most of the observed nanoparticles evolved directly from ions and charged clusters. The simulated sulfuric acid vapor, ultrafine aerosol, and condensation nuclei (CN) concentrations are all consistent with field measurements in this case. We also find that ion-induced nucleation makes its greatest contribution when ambient ionization rates are relatively low, background aerosol surface area densities are small, and H_2SO_4 vapor concentrations are elevated (but not extreme). In these circumstances, CN formation is limited, and is modulated by the ionization rate.

It is further demonstrated that neutral clusters apparently grow too slowly to explain the particle burst observed during the PEM mission, owing to relatively weak interactions between vapor molecules and small clusters. Indeed, classical binary (H_2SO_4/H_2O) homogeneous nucleation theory would not have predicted any particle formation under the prevailing field conditions. Other simulations carried out assuming that neutral sulfate clusters are stable under all conditions, and experience perfect accommodation for all vapor and particle collisions (i.e., a unit sticking coefficients) fail to reproduce either the measured aerosol (ultrafine and condensation nuclei) concentrations or acid vapor abundances. We conclude from these results that the accommodation coefficients for collisions between acid molecules and small neutral acid/water clusters must be significantly smaller than unity. Accordingly, none of the present simulations support the possibility of a significant contribution from alternative homogeneous nucleation processes (e.g., ternary nucleation involving ammonia as well as sulfuric acid and water [*Kulmala et al.*, 2000]) for the conditions studied.

The potential influence of GCR flux modulation by solar activity was simulated for a 25% change in the background GCR ionization rate (which is a typical range over the 11-year solar cycle). Under MBL conditions corresponding to the nucleation event studied above, our simulations indicate that GCR variations could lead to a maximum change of ~16% in the number of ultrafine particles larger than 3 nm diameter. This perturbation would occur within a few hours of the onset of nucleation but would subsequently decay over time to ~7-8% after 8 hours. For condensation nuclei >10 nm in size a maximum 9% increase occurs after a few hours, slowly dropping to ~7% after 8 hours. At longer times the decay in the perturbation would be expected to continue. While the number of new aerosols that survive to form CCN has not been determined here, it is certain to be influenced by the competition between scavenging and growth controlled by preexisting aerosols and condensable vapors, especially sulfates and organic compounds.

Accordingly, the apparent influence of ionization rates on aerosol formation noted in this work cannot be directly related to putative changes in CCN populations and cloud properties. Nevertheless, GCR-driven IMN may represent the first step in a viable physical mechanism that underlies the inferred correlation between variations in global cloud properties and the solar cycle. To be sure, there are many other factors affecting aerosol formation and growth in addition to the ionization rate that have not been considered here, including the identities and abundances of precursor vapors, and the compositions and surface areas of background aerosols. Moreover, simplified analytical approaches to the problem [*Turco et al.*, 2000], which seem to capture the strong nonlinear behavior of this coupled ion, aerosol, vapor system as seen in the present simulations, imply relatively low sensitivity of long-term aerosol populations to GCR variations.

Obviously, a number of additional laboratory and field measurements, as well as theoretical studies will be needed to advance the theory of ion-mediated aerosol formation, and to define the role of galactic cosmic radiation in Earth's climate. Simultaneous in situ measurements of ion mobility spectra, ultrafine particle size distributions, charged aerosol fractions, and precursor vapor concentrations during a major nucleation event would be useful in verifying models. The implementation of Lagrangian experiments could also be fruitful, eliminating the confounding effects of air mass changes. The main uncertainty in the kinetic-based simulations presented here relates to the size-dependent charge effects on coagulation kernels, accommodation coefficients, and cluster dissociation rates, especially for interactions involving subnanometer molecular aggregates. Crucial to this work will be laboratory studies that can provide thermodynamic data for simulating the kinetics of ion clustering in the early stages of particle formation. Finally, if an ionization/cloud/climate connection is to be made, the complex microphysics of aerosol/cloud interactions must be further clarified.

Acknowledgments: NASA funded this work under grants NAG1-1899 and NAG5-2723 and the NSF under grants ATM96-18425 and ATM00-70847.

References

Aikin, A. C., and W. D. Pesnell, Uptake coefficient of charged aerosols–implications for atmospheric chemistry, *Geophys. Res. Lett.*, *25*, 1309-1312, 1998.

Alam, M. K., The effect of van der Waals and viscous forces on aerosol coagulation, *Aerosol Sci. Tech.*, *6*, 41-52, 1987.

Aplin, K. L., and R. G. Harrison, A computer-controlled Gerdien atmospheric ion counter, *Rev. Sci. Instrum.*, *71*, 3037-3041, 2000.

Arnold, F., Multi-ion complexes in the stratosphere—Implications for trace gases and aerosol, *Nature*, *284*, 610-611, 1980.

Arnold, F., J. Schneider, K. Gollinger, H. Schlager, P. Schulte, D. E. Hagen, P. D. Whitefield and P. van Velthoven, Observations of upper tropospheric sulfur dioxide- and acetone-pollution: Potential implications for hydroxyl radical and aerosol formation, *Geophys. Res. Lett.*, *24*, 57-60, 1997.

Arnold, F., T. Stilp, R. Busen and U. Schumann, Jet engine exhaust chemiion measurements: Implications for gaseous SO_3 and H_2SO_4, *Atmos. Environ.* *32*, 3073-3077, 1998a.

Arnold, F., K.-H. Wohlfrom, M. W. Klemm, J. Schneider, K. Gollinger, U. Schumann and R. Busen, First gaseous ion composition measurements in the exhaust plume of a jet aircraft in flight: Implications for gaseous sulfuric acid, aerosols, and chemiions, *Geophys. Res. Lett.* *25*, 2137, 1998b.

Arnold, F., et al., Detection of massive negative chemiions in the exhaust plume of a jet aircraft in flight. *Geophys. Res. Lett.* *26*, 1577, 1999.

Arnold, F., A. Kiendler, V. Wiedemer, S. Aberle, and T. Stilp, Chemiion concentration measurements in jet engine exhaust at the ground: Im-

plications for ion chemistry and aerosol formation in the wake of a jet aircraft, *Geophys. Res. Lett.*, *27*, 1723-1726, 2000.

Capaldo, K. P., P. Kasibhatla, and S. N. Pandis, Is aerosol production within the remote marine boundary layer sufficient to maintain observed concentrations? *J. Geophys. Res.*, *104*, 3483-3500, 1999.

Castleman, A. W., Jr., Nucleation and molecular clustering about ions, *Adv. Colloid Interface Sci.*, *10*, 73-128, 1979.

Castleman, A. W., Jr., P. M. Holland, and R. G. Keesee, The properties of ion clusters and their relationship to heteromolecular nucleation, *J. Chem. Phys.*, *68*, 1760-1767, 1978.

Charlson, R. J., S. E. Schwartz, J. M. Hales, R. D. Cess, J. A. Coakley, Jr., J. E. Hansen, and D. J. Hofmann, Climate forcing by anthropogenic aerosols, *Science*, *255*, 423-430, 1992.

Clarke, A. D., et al., Particle nucleation in the tropical boundary layer and its coupling to marine sulfur sources, *Science*, *282*, 89, 1998.

Clarke, A. D., F. Eisele, V. N. Kapustin, K. Moore, et al., Nucleation in the equatorial free troposphere: Favorable environments during PEM-Tropics, *J. Geophys. Res.*, *104*, 5735-5744, 1999.

Coffman, D. J., and D. A. Hegg, A preliminary study of the effect of ammonia on particle nucleation in the marine boundary layer, *J. Geophys. Res.*, *100*, 7147-7160, 1995.

Covert, D. S., V. N. Kapustin, P. K. Quinn, and T. S. Bates, New particle formation in the marine boundary layer, *J. Geophys. Res.*, *97*, 20,581-20,589, 1992.

Davis, D., et al., Dimethyl sulfide oxidation in the equatorial Pacific: Comparison of model simulations with field observations for DMS, SO_2, H_2SO_4 (g), MSA(g), MS, and NSS, *J. Geophys. Res.*, *104*, 5765-5784, 1999.

Eisele, F. L., and D. R. Hanson, First measurement of prenucleation molecular clusters, *J. Phys. Chem.*, *104*, 830-836, 2000.

Fehsenfeld, F. C., I. Dotan, D. L. Albritton, C. J. Howard, and E. E. Ferguson, Stratospheric positive ion chemistry of formaldehyde and methanol, *J. Geophys. Res.*, *83*, 1333-1336, 1978.

Feynman, J., and A. Ruzmaikin, Modulation of cosmic ray precipitation related to climate, *Geophys. Res. Lett.*, *26*, 2057-2060, 1999.

Fuchs, N. A., *The Mechanics of Aerosols*, edited by C. N. Davies, Macmillan, New York, 1964.

Gamero-Castaño M., and J. Fernández de la Mora, A condensation nucleus counter (CNC) sensitive to singly charged sub-nanometer particles, *J. Aerosol Sci.*, *31*, 757-772, 2000.

Hamill, P., R. P. Turco, C. S. Kiang, O. B. Toon, and R. C. Whitten, An analysis of various nucleation mechanisms for sulfate particles in the stratosphere, *J. Aerosol Sci.*, *13*, 561-585, 1982.

Hoppel, W. A., and G. M. Frick, Ion-aerosol attachment coefficients and the steady-state charge distribution on aerosols in a bipolar ion environment, *Aerosol Sci. Tech.* *5*, 1-21, 1986.

Hoppel, W. A., G. M. Frick, J. W. Fitzgerald, and R. E. Larson, Marine boundary layer measurements of new particle formation and the effects nonprecipitating clouds have on aerosol size distribution, *J. Geophys. Res.*, *99*, 14,443-14,459, 1994.

Hõrrak, U., J. Salm, and H. Tammet, Burst of intermediate ions in atmospheric air, *J. Geophys. Res.*, *103*, 13,909-13915, 1998.

Hõrrak, U., J. Salm, and H. Tammet, Statistical characterization of air ion mobility spectra at Tahkuse Observatory: Classification of air ions, *J. Geophys. Res.*, *105*, 9291-9302, 2000.

Huertas, M. L., A. M. Marty, and J. Fontan, On the nature of positive ions of tropospheric interest and on the effect of polluting organic vapors, *J. Geophys. Res.*, *79*, 1737-1743, 1974.

Ianni, J. C., and A. R. Bandy, A theoretical study of the hydrates of $(H_2SO_4)_2$ and its implications for the formation of new atmospheric particles, *Theochem*, *497*, 19-37, 2000.

Intergovernmental Panel on Climate Change, *Climate Change 1995: The Science of Climate Change, Intergovernmental Panel on Climate Change*, edited by J. T. Houghton et al., Cambridge Univ. Press, New York,1996.

Jacobson, M. Z., and R. P. Turco, Simulating condensational growth, evaporation and coagulation of aerosols using a combined moving and stationary size grid, *Aerosol Sci. Tech.*, 22, 73-92, 1995.

Jacobson, M. Z., A. Tabazadeh, and R. P. Turco, Simulating equilibrium within aerosols and nonequilibrium between gases and aerosols, *J. Geophys. Res.*, *101*, 9079-9091, 1996.

Kärcher, B., F. Yu, F. P. Schroeder, and R. P. Turco, Ultrafine aerosol particles in aircraft plumes: Analysis of growth mechanisms, *Geophys. Res. Lett.*, *25*, 2793-2796, 1998.

Kernthaler, S. C., R. Toumi, and J. D. Haigh, Some doubts concerning a link between cosmic ray fluxes and global cloudiness, *Geophys. Res. Lett.*, *26*, 863-865, 1999.

Korhonen, P., M., et al., Ternary nucleation of H_2SO_4, NH_3, and H_2O in the atmosphere, *J. Geophys. Res.*, *104*, 26,349-26,353, 1999.

Kuang, Z. M., Y. B. Jiang, and Y. L. Yung, Cloud optical thickness variations during 1983-1991: Solar cycle or ENSO? *Geophys. Res. Lett.*, *25*, 1415-1417, 1998.

Kulmala, M., A. Laaksonen, and L. Pirjola,Parameterizations for sulfuric acid/water nucleation rates, *J. Geophys. Res.*, *103*, 8301-8307, 1998.

Kulmala, M., L. Pirjola, and J. M. Mäkelä, Stable sulphate clusters as a source of new atmospheric particles, *Nature*, *404*, 66-69, 2000.

Loeb, L. B., *Basic Processes of Gaseous Electronics*, Chap. VI, Univ. of Calif. Press, Berkeley, 1960.

Lovejoy, E. R., Ion trap studies of $H^+(H_2SO_4)_m(H_2O)_n$ reactions with water, ammonia, and a variety of organic compounds, *Int. J. Mass Spectrom.*, *191*, 231-241, 1999.

Marlowe, W. H., Derivation of aerosol collision rates for singular, attractive contact potentials, *J. Chem. Phys.*, *73*, 6284-6287, 1980a.

Marlowe, W. H., Lifshitz-van der Waals forces in aerosol particle collisions: Introduction—water droplets, *J. Chem. Phys.*, *73*, 6288-6295, 1980b.

Marsh, N., and H. Svensmark, Cosmic rays, clouds, and climate, *Space Sci. Rev.*, in press, 2000.

Menzel, W. P., D. P. Wylie, and K. I. Strabala, Seven years of global cirrus cloud statistics using HIRS, in *IRS96: Current Problems in Atmospheric Radiation*, edited by W. L. Smith and K. Stamnes, pp. 719-725, A. Deepak, Hampton, Va, 1997.

Mohnen, V. A., Discussion of the formation of major positive and negative ions up to the 50 km level, *Pure Appl. Geophys.*, *84*, 141-153, 1971.

Mohnen, V. A., Stratospheric ion and aerosol chemistry and possible links with cirrus cloud microphysics: A critical assessment, *J. Atmos. Sci.*, 47, 1933-1948, 1990.

Pruppacher, H. R., and J. D. Klett, *Microphysics of Clouds and Precipitation*, D. Reidel, Norwell, Mass., 1978.

Pudovkin, M. I., and S. V. Veretenenko, Cloudiness associated with Forbush-decreases of galactic cosmic rays, *J. Atmos. Terr. Phys.*, *57*, 1349-1355, 1995.

Raes, F., J. Augustin, and R. Vandingenen, The role of ion-induced aerosol formation in the lower atmosphere, *J. Aerosol Sci.*, *17*, 466-470, 1986.

Raes F., A. Saltelli, and R. Vandingenen, Modelling formation and growth of H_2SO_4-H_2O aerosols–uncertainty analysis and experimental evaluation. *J. Aerosol Sci.*, *23*, 759-771, 1992.

Reischl, G. P., J. M. Mäkelä, R. Karch, and J. Necid, Bipolar charging of ultrafine particles in the size range below 10 nm, *J. Aerosol Sci.*, *27*, 931-949, 1986.

Reiter, R., *Phenomena in Atmospheric and Environmental Electricity*, Elsevier, New York, 1992.

Russell, L. M., S. N. Pandis, and J. H. Seinfeld, Aerosol production and growth in the marine boundary layer, *J. Geophys. Res.*, *99*, 20,989-21,003, 1994.

Shindell, D., D. Rind, N. Balachandran, J. Lean, and P. Lonergan, Solar cycle variability, ozone, and climate, *Science*, *284*, 305-308, 1999.

Soon, W., S. Baliunas, E. S. Posmentier, and P. Okeke, Variations of solar coronal hole area and terrestrial lower tropospheric air temperature from 1979 to mid-1998: Astronomical forcings of change in Earth's climate?, *New Astron.*, 4, 563-579, 2000.

Svensmark, H., Influence of cosmic rays on Earth's climate, *Phys. Rev. Lett. 81*, 5027, 1998.

Svensmark, H., and E. Friis-Christensen, Variation of cosmic ray flux and global cloud coverage–A missing link in solar-climate relationships, *J. Atmos. Sol. Terr. Phys.*, *59*, 1225, 1997.

Svensmark, H., and E. Friis-Christensen, Reply to comments on "Variation of cosmic ray flux and global cloud coverage—A missing link in solar–climate relationships," *J. Atmos. Sol. Terr. Phys.*, *62*, 79-80, 2000.

Tammet H., and S. Israelsson, Atmospheric electricity as a factor of dry deposition of particulate pollution, in Proceeding of *11th International Conference on Atmospheric Electricity, NASA Conf. Publ., CP—1999-209*, 261, 1999.

Tinsley, B. A., Correlations of atmospheric dynamics with solar wind-induced changes of air-Earth current density into cloud tops, *J. Geophys. Res.*, *101*, 29,701-29,714, 1996.

Tinsley, B. A., Influence of solar wind on the global electric circuit, and inferred effects on cloud microphysics, temperature, and dynamics in the troposphere, *Space Sci. Rev.*, in press, 2000.

Turco, R. P., and F. Yu, Aerosol formation in the troposphere, in *Proc.*

NATO ASI, Ozone and Aerosols, Kolympari, Crete, May 15-24, 1999, in press, 2000.

Turco, R. P., P. Hamill, O. B. Toon, R. C. Whitten, and C. S. Kiang, A one-dimensional model describing aerosol formation and evolution in the stratosphere, Part I, Physical processes and mathematical analogs, *J. Atmos. Sci., 36*, 699–717, 1979.

Turco, R. P., J.-X. Zhao, and F. Yu, A new source of tropospheric aerosols: Ion-ion recombination, *Geophys. Res. Lett., 25*, 635-638, 1998.

Turco, R. P., F. Yu, and J.-X. Zhao, Tropospheric sulfate aerosol formation via ion-ion recombination, *J. Air Waste Manag. Assoc., 50*, 902-907, 2000.

Twomey, S., *Atmospheric Aerosols*, Elsevier, New York, 1977.

Viggiano, A. A., In-situ mass-spectrometry and ion chemistry in the stratosphere and troposphere, *Mass Spectrom. Rev., 12*, 115-137, 1993.

Viggiano, A. A., R. A. Perry, D. L. Albritton, E. E. Ferguson, and F. C. Fehsenfeld, The role of H_2SO_4 in stratospheric negative-ion chemistry, *J. Geophys. Res., 85*, 4551-4555, 1980.

Viggiano, A. A., F. Dale, and J. F. Paulson, Proton transfer reactions of $H^+(H_2O)_{n=2-11}$ with methanol, ammonia, pyridine, acetonitrile, and acetone, *J. Chem. Phys., 88*, 2469-2477, 1988.

Weber, R. J., P. H. McMurry, F. L. Eisele, and D. J. Tanner, Measurement of expected nucleation precursor species and 3-500-nm diameter particles at Mauna Loa Observatory, Hawaii. *J. Atmos. Sci., 52*, 2242-2257, 1995.

Weber, R. J., J. J. Marti, P. H. McMurray, F. L. Eisele, D. J. Tanner, and A. Jefferson, Measured atmospheric new particle formation rates: Implications for nucleation mechanisms. *Chem. Eng. Comm., 151*, 53-62, 1996.

Weber, R. J., J. J. Marti, P. H. McMurry, F. L. Eisele, D. J. Tanner, and A. Jefferson, Measurement of new particle formation and ultrafine particle growth rates at a clean continental site. *J. Geophys. Res., 102*, 4375-4385, 1997.

Weber, R. J., et al., A study of new particle formation and growth involving biogenic and trace gas species measured during ACE 1, *J. Geophys. Res., 103*, 16,385-16,396, 1998.

Weber, R. J., et al., New particle formation in the remote troposphere: A comparison of observations at various sites, *Geophys. Res. Lett., 26*, 307-310, 1999.

Wohlfrom, K.-H., S. Eichkorn, F. Arnold, and P. Schulte, Massive positive and negative ions in the wake of a jet aircraft: Detection by a novel aircraft-based mass spectrometer with a large mass range, *Geophys. Res. Lett., 27*, in press, 2000.

Wyslouzil, B. E., J. H. Seinfeld, R. C. Flagan, and K. Okuyama, Binary nucleation in acid-water systems, II, Sulfuric-acid-water and comparison with methanesulfonic acid-water, *J. Chem. Phys., 10*, 6842-6850, 1991.

Yu, F., A study of the formation and evolution of aerosols and contrails in aircraft wakes: Development, validation and application of an advanced particle microphysics (APM) model. Ph.D. thesis, Univ. of Calif., Los Angeles, 1998.

Yu, F., and R. P. Turco, The role of ions in the formation and evolution of particles in aircraft plumes, *Geophys. Res. Lett., 24*, 1927-1930, 1997.

Yu, F., and R. P. Turco, The formation and evolution of aerosols in stratospheric aircraft plumes: Numerical simulations and comparisons with observations, *J. Geophys. Res., 103*, 25,915-25,934, 1998.

Yu, F., and R. P. Turco, Evolution of aircraft-generated volatile particles in the far wake regime: Potential contributions to CCN/IN, *Geophys. Res. Lett., 26*, 1703-1706, 1999.

Yu, F., and R. P. Turco, Ultrafine aerosol formation via ion-mediated nucleation, *Geophys. Res. Lett., 27*, 883-886, 2000a.

Yu, F., and R. P. Turco, On the contribution of lightning to ultrafine aerosol formation, *Geophys. Res. Lett.*, in press, 2000b.

Yu, F., R. P. Turco, B. Kärcher, and F. P. Schröder, On the mechanisms controlling the formation and properties of volatile particles in aircraft wakes, *Geophys. Res. Lett., 25*, 3839-3842, 1998.

Yu, F., R. P. Turco, and B. Kärcher, The possible role of organics in the formation and evolution of ultrafine aircraft particles, *J. Geophys. Res., 104*, 4079-4087, 1999.

R. P. Turco, Department of Atmospheric Sciences, University of California, Los Angeles, CA 90095-1565. (turco@atmos.ucla.edu)

F. Yu, Atmospheric Sciences Research Center, State University of New York at Albany, 251 Fuller Road, Albany, New York 12203. (yfq@asrc.cestm.albany.edu)

(Received May 31, 2000; revised August 29, 2000;
accepted August 31, 2000.)